Stratigraphic evolution and characteristics of lobes: a high-resolution study of Fan 3, Tanqua Karoo, South Africa.

by

J.M. Neethling

Thesis presented in partial fulfilment of the requirements for the degree of

Master of Science

at the University of Stellenbosch

Supervisors

Dr. H. de V. Wickens

Dr. D.M. Hodgson

March 2009

Geology

Stellenbosch University

Declaration

By submitting this thesis electronically, I declare that the entirety of the work contained therein is my own, original work, that I am the owner of the copyright thereof (unless to the extent explicitly otherwise stated) and that I have not previously in its entirety or in part submitted it for obtaining any qualification.

_____

Jacobus Martinus Neethling

Date: 10 November 2008

Abstract

Fan 3 is one of four basin-floor fans that form part of the Tanqua Karoo Fan Complex in South Africa. It can be subdivided into several sandstone lobes, based on the presence of thin-bedded siltstone intervals above and below major sandstone packages. Six lobes are identified in the mid fan section, as well as two older groups of thin, low-volume turbidite deposits at the base. Some of the lobes are further divided into an upper and lower lobe-element based on depositional behaviour. The volumetrically and spatially larger lobes have a finger-like appearance in plan view, which is attributed to multiple lobe-scale axial zones. This is especially visible towards the eastern margins of Lobes 2, 4 and 5. The stratigraphy and facies distribution are presented on several 2D panels. Computer generated isopach maps are presented for each lobe, lobe-element and interlobe unit.

Autogenic control on the depositional pattern of the Fan 3 lobe complex was inferred from the palaeoflow patterns of the composing lobes and lobe-elements. The majority of the lobes show a north-eastern palaeoflow direction in the south, with a gradual westward shift in the north. Inferred controls are basin-floor topography, the presence of pre-existing lobes, and characteristics of the depositional flow, such strength, density, sediment load, palaeoflow direction.

The progradational to retrogradational stacking pattern of Fan 3 could also be interpreted to be the result of allogenic control, where each lobe was deposited during a period of relative sea-level lowstand, followed by a brief flooding period dominated by silt deposition. The continuity of the latter contributes to this interpretation.

The results of the depositional model suggest that each lobe displays different depositional patterns. A single depositional model therefore cannot describe the whole of Fan 3, and a combination of autogenic and allogenic controls were likely affecting the deposition of Fan 3.

Fan 3 outcrops along the southern Gemsbok River valley represents a strike section that can be used as an analogue for the channelised sheet to sheet deposit transition. The basic pattern for the deposition of the lobes of Fan 3 is channels in the proximal sections, going into lobe-scale

channelised sheets as the flow became distributive in the frontal splay. Sheet deposits are bed-set scale bodies and are present in areas removed from channelised zones, i.e. either from the axial zone to the lobe fringe, or between axial zones.

The computer modelling done in Schlumberger's Petrel was conducted in order to determine if the data gathered could be used effectively for computer simulations and static modelling. The linear nature of the outcrop data, however, does not provide a sufficient three-dimensional spread of data, making the use of these data in computer simulation difficult. With more information from behind outcrop sources, such as core or subsurface imagery, the data could probably be used to greater effect.

Keywords: Lobes, axial zones, finger-shaped deposits

Acknowledgements

My sincerest thanks to Dr. H. DeV. Wickens for the opportunity he has given me in conducting this study. His guidance and support over the past two years have been invaluable. I would also like to thank Dr. Dave Hodgson (University of Liverpool) for taking time out of his busy schedule to provide guidance and insight into the project, and for the opportunity to present this project at the AAPG 2008 conference in Cape Town. His help in the field also proved invaluable during the four months of fieldwork. On that note, a special thanks go to Amandine Prélat for the help she offered while she was in South Africa for her own PhD's fieldwork.

As part of the Lobe project, funding for this project came from a consortium of international petroleum companies, namely Chevron, Total, Petrobras, Maersk Oil, Shell, Statoil-Hydro and PetroSA.

I am grateful to Schlumberger for allowing a fellow student and myself the use of Petrel. Brian Cockrell (Schlumberger) deserves great thanks, as he is the one who organised it and got us going with the basics of Petrel. PetroSA, and in no small part Jody Frewin, are also thanked for the use of their powerful computer running Petrel, and for their organisation with Schlumberger.

Jody Frewin cannot be thanked enough. Without her help and interest (and some weekends), the Petrel work would never have been realised.

I would like to thank Frank Willemse for allowing us to stay in his farmhouse of Kleine Gemsbok Fontein. I grew quite fond of the place. Also, thanks to all the farmers on whose farms the study was conducted.

And last, but most certainly not least, my family and friends.

Table of Contents

Abstract ..... **i**

Acknowledgements ..... **iii**

Table of Contents **1**

List of Figures **3**

Chapter 1 ..... **10**

Introduction 11
1.1 General 11
1.2 Previous work 12
1.3 Aims of this study 13
1.4 Geological Setting 15
1.4.1 Geology of the area 15
1.5 Methods and Materials 20

Chapter 2 ..... **24**

A brief review of deep-water sedimentation 25
2.1 Introduction 25
2.2 Sediment gravity flow 25
2.2.1 Slides and slumps 25
2.2.2 Debris flows 26
2.2.3 Grain flows 26
2.2.4 Liquefied flows 26
2.2.5 Turbidity flows 26
2.3 Deposits of turbidity flows 27
2.3.1 Introduction 27
2.3.2 Deposits formed by turbidity flows 27
2.3.3 Models of turbidite deposition 27
2.4 Terminology 29

Chapter 3 ..... **30**

Sedimentology, Stratigraphy and Architecture of Fan 3 31
3.1 Geology of Fan 3 31
3.2 Lithofacies 31
3.2.1 Lithofacies 1: Claystone 31
3.2.2 Lithofacies 2: Parallel- and ripple cross–laminated siltstone 32
3.2.3 Lithofacies 3: Structureless sandstone 34
3.2.4 Lithofacies 4: Structured sandstone 39
3.2.5 Lithofacies 5: Mud-clast conglomerates 43
3.3 Stratigraphy 44
3.3.1 Introduction 44
3.3.2 Stratigraphy of Fan 3 in the study area 45
3.4 Architecture 49
3.4.1 Introduction 49
3.4.2 Architecture of mid-fan Fan 3 60

Chapter 4 ..... **68**

Application of Sequence Stratigraphy 69
4.1 Introduction 69
4.2 Application 71
Chapter 5 75

Data Manipulation 76
5.1 Introduction 76
5.2 Digitisation of data 76
Chapter 6 81

Deposition of Fan 3 82
6.1 Introduction 82
6.2 Finger-shaped deposits of Fan 3 83
6.3 Isopach maps 85
6.4 Discussion 88
6.4.1 Lobe formation 88
6.4.1 Lobe stacking 91
Chapter 7 94

Data Modelling with Petrel 95
7.1 Introduction 95
7.2 Petrel Modelling 96
7.2.1 Field size 97
7.2.2 Logs and correlation 98
7.2.3 Surfaces 98
7.2.4 Grids, Zones and Layering 103
7.2.5 Facies modelling 104
7.2.6 Limitations encountered during modelling in Petrel 113
7.3 Results 113
Chapter 8 116

Conclusions 117
8.1 High resolution outcrop maps and data incorporation 117
8.2 Channelised lobe to sheet deposit transition 118
8.3 Conceptual depositional model 118
8.4 Computer modelling with Petrel 119
References 121

Appendix A 130

AAPG Poster 131
Appendix B 137

PetroSA Presentation 138
Appendix C 145

Petrel Thickness Maps 146
Appendix D 163

Petrel Correlation Panels 164
Appendix E 169

Interpolation Algorithms in Petrel 170

List of Figures

Figure 1.1 A simplified geological map of South Africa to show the location of the Tanqua sub-basin (Geological map, Council for Geoscience, 2000). The Laingsburg and Tanqua sub-basins can be seen in (B). The yellow area in (C) represents the total outcrop of the Skoorsteenberg Formation in the Tanqua sub-basin. 17

Figure 1.2 A diagram illustrating the location of the Ecca Group in the stratigraphy of the Cape-Karoo Succession (Wickens, 1994)..... 18

Figure 1.3 Outcrop distribution diagram of the Tanqua Fan Complex with Fan 3 highlighted to show the extent of its outcrop. The red block represents the study area, displayed in figure 1.5. Several panoramic photos have also been added to illustrate the appearance of Fan 3 at selected points of outcrop. Note the stacked channel-fills at the base-of-slope setting at the Ongeluks River. The mid-fan area displays several amalgamated zones, but no true channels. Distal outcrop becomes very thin, with almost no indications of channelised flows. (adapted from Wickens, 1994)..... 19

Figure 1.4 Locations of the south Gemsbok River valley outcrops in relation to a depositional diagram for fine-grained turbidites. The red line represents the oblique strike section of the southern Zoet Meisjies Fontein 75 and Rondavel 34 outcrops, and the red line the dip-sections of the Los Kop 74 and Krans Kraal 83 outcrops. Modified from Bouma (2000). 20

Figure 1.5 Triangle discribing the use of the formula($x^2 = y^2+z^2-2yz\ cos\ \Theta$) to triangulate distances between profiles. x, y and z represent the distances between the profiles..... 21

Figure 1.6 Google Earth (2008) satellite image of the study area, indicating the dimensions and location of the field area. 22

Figure 1.7 Topographic map of the study area. The red dots represent the positions of the measured vertical profiles..... 23

Figure 2.1 A summary diagram of the Lowe (1982), Bouma (1962) and Stow and Shanmugam (1980) subdivisions for turbidites (from Shanmugam, 2000). 29

Figure 3.1 An example of the siltstone to claystone relation close to the base of the succession. This relation is only present at the base and top of Fan 3, as no claystones are present within the fan succession. 32

Figure 3.2 Alternating relationship between coarse- and fine-grained siltstone that is present throughout the study area. This relationship forms the most common breaks between lobes. They are commonly referred to simply as thin-bedded intervals. 33

Figure 3.3 An example of the general appearance of structureless sands in the study area. This particular section is located in one of several highly amalgamated channelised areas, with sandstone cliffs reaching 10 metres or more in thickness. Note person for scale underneath the overhang (circle). 35

Figure 3.4 Example of the dewatering features found in structureless sands. Here the smaller linear features are present, as well as a much larger dewatering pipe with significant alteration along its edges. 36

Figure 3.5 Groove marks at the base of a structureless sandstone. These marks infer the general orientation of palaeocurrents. 37

Figure 3.6 Example of a rip-up clast near the base of a thick sandstone unit. This example is near the base of Fan 3, close to the eastern margin of the fan. 38

Figure 3.7 An example of a particularly large calcareous concretion. Note the concentric growth pattern. 38

Figure 3.8 An example of where the transition between Ta and Tb is not particularly clear-cut. The transition only becomes apparent laterally. This particular feature is fairly common along the Gemsbok River outcrop. 39

Figure 3.9 An example of the sharp transition between a Tb and Tc succession. 41

Figure 3.10 Closer views of ripple cross-laminated sandstone: (A) Ripple cross-lamination; (B) Climbing ripple-lamination. 42

Figure 3.11 This is how mud-clast conglomerates mostly appear in the study area. This example lies at the base of a large structureless sand, the latter loading into the MCC. 43

Figure 3.12 Hierarchy of depositional elements in distributive deep-water systems. The division consists of four scales of elements, namely single beds, lobe-elements, lobes and the lobe complex (or fan) defined by the bounding fine-grained units and mappable extent, not thickness. Lobes are separated by interlobe units of fine-grained, thin-bedded siltstones (From Lobe Field Guide, © STRAT Group, University of Liverpool, June 2008). 44

Figure 3.13 A representative profile (J0820250LK) to show the stratigraphy of Fan 3. Sub Lobe 2 has already pinched out. (A) shows the appearance of Lobe 6 at this profile location. It is less than a metre thick. (B) shows the appearance of Lobe 2, 4 and Lower Lobe 5. 48

Figure 3.14 Legend for all the correlation panels. 50

Figure 3.15 Topographical map of the area indicating the locations of the various correlation panels. 51

Figure 3.16 Panel 1 - 2. Fan 3 disappears into the ground a few hundred metres to the east of the last profile. 52

Figure 3.17 Panel 3. The most continuous section of outcrop in the field area is the first 2.3 kilometres to the west of this area. It represents the southern Gemsbok River Valley outcrop of mid-fan Fan 3. 53

Figure 3.18 Panel 3 - 4. This section of outcrop lies slightly to the south of Panel 3. The two edge profiles are part of Panel 3.The western correlation with Fan 3 can be walked out. 54

Figure 3.19 Panels 5 and 6. They represent the first two valleys south of the Gemsbok valley. From Panel 5 onwards it becomes increasingly difficult to correctly correlate the Panels, as the outcrops become poorer and further apart. 55

Figure 3.20 Panel 7. Panel 7 is not truly a "straight line correlation, but rather a correlation around a bend in the outcrop. The two sides of the headland were close enough together to warrant the above correlation. 56

Figure 3.21 Panel 8 - 9. The Los Kop twins (bottom photo) are situated some three kilometres away from the nearest correlatable outcrop to the east. As such the only a general correlation could be safely attempted. 57

Figure 3.22 Panel 10 - 11. The southern most strike section. Again, most of the outcrop is located on isolated hills several hundred metres from the nearest correlatable outcrop. 58

Figure 3.23 Panel 12. A 4.9 kilometre north-south trending dip-section from mid-fan (north) to more proximal (south). 59

Figure 3.24 Averaged palaeoflow directions measured for Fan 3 in previous studies. From Hodgson *et al.* (2006) 60

Figure 3.25 Palaeoflow directions for Fan 3. (A) is a summary of the whole Fan 3, whereas (B) breaks down the palaeoflow into the main lobes. The yellow blocks represent the areas from which the groups of palaeoflow indicators were taken. The majority of the palaeoflow indicators are ripple laminations. 61

Figure 4.1 A simple diagram from Sixsmith (2000) showing the surfaces and zones used to describe a turbidite. 70

Figure 4.2 Application of sequence stratigraphy on the outcrops of Fan 3 of the southern Gemsbok River valley. 72

Figure 4.3 Schematic of a dip section through mid to distal Fan 3 to illustrate the different stages of deposition. Modified from Prélat *et al*. (in review). 73

Figure 5.1 Part of one of the spreadsheets used to calculate top and base values for use in Petrel. The yellow cells represent areas where no data were present in the initial construction of the spreadsheet. The values were calculated during the later stages of modelling in order to facilitate the process in Petrel. 77

Figure 5.2 An example of how DSL (left) and CorelDraw (right) displays the same vertical profile, in this case J4930008LK. DSL's digital usage of data makes it very useful for exporting into other programs, whereas CorelDraw provides a better visual display of the data. 78

Figure 6.1 Three depositional models for turbidity currents as suggested by Machado et al. (2004). These models are based on age and complexity. Initially, a turbidity current forms a bulb. Given time and a constant sediment supply, several bulbs can build a lobe. 82

Figure 6.2 Example of the bedded nature of the finger-shaped axial zones. The correlated section at the top can be traced for hundreds of meters along strike, whereas the "extra" section at the base is very localised, with less than a hundred metres lateral extent. Note the large amount of mud-clast conglomerates at the top of the thickest sandstone. Here it resembles a debrite, with significant amounts of organic material. 83

Figure 6.3 Example of the plastic (soft-sediment) deformation observed in the units below a finger-shaped axial zone. This example is a siltstone located in the claystones about 2 meters below a significantly thickened lobe (Upper Lobe 4). 84

Figure 6.4 Example of the difference between the first isopach maps and the final product. Both represent Lower Lobe 5. (A) used the old, larger polygon, and the colour scales were automatically adjusted to the minimum and maximum values. (B) used the constrained polygon and the colour scale was manually set to 10 metres. The results may appear similar, but there are some significant differences: (B) has a much smaller degree of contouring. The purple in (B) is both a result of outcrop not revealing the whole of the lobe (in the west and south), as well as true thinning (east). 86

Figure 6.5 Example of isopach maps in relation to a vertical profile, as well as the axial positions of all lobes, determined from the isopach maps and field data (Chapter 3). Also provided on the axis map is the location of the boundary polygon in order to gain perspective on the location of the isopach maps. The yellow circles on the isopach maps represent the location of the example profile. 87

Figure 6.6 Schematic of the structure of a lobe. The diagram illustrates the transition from channel to channelised sheets, and channelised sheets to sheets. The single axial zone is the transition zone from confined flow to unconfined floor spreading. Also indicated is the position of the southern Gemsbok Valley outcrop in relation to Lobes 2, 4, 5 and 6. 89

Figure 6.7 Schematic to illustrate the strike section stacking pattern of Fan 3 in the mid-fan area (southern Gemsbok River valley) The red line represents the western end of outcrop in the valley. Not to scale. 91

Figure 6.8 Schematic of the probable locations of the Lobes in order to illustrate their positions relative to each other. Also shown is the inferred stepping pattern for the lobes. The black arrows represent basinward stepping (progradation), the yellow arrows represent aggradation, and the red arrows represent back stepping. 93

Figure 7.1 A 3D view in Petrel, looking north, of the wells and well-tops used. These data represent all 72 vertical profiles (wells). 96

Figure 7.2 Example window of how data appear when imported from text files into Petrel. 97

Figure 7.3 The different polygons used in various runs in Petrel. The constrained polygon was used for the final product. 100

Figure 7.4 Two of the initial surfaces created in Petrel. (A) used the Kriging algorithm, whereas the Convergent Interpolation (CI) algorithm was used for (B). Note the difference in surface shape between the two methods: Kriging created a much smoother surface but was unable to keep to the data, whereas CI managed to honour the data points to an acceptable degree. 102

Figure 7.5 This figure shows the zones created in the first grid run. The surfaces created from the larger polygons caused some major pinch-out features when grouped together. One of the reasons for this is because they used different polygons, and as such the Z values could not be correctly adjusted. 103

Table 7.1 Summary table of the lithofacies used. The DSL lithofacies were grouped in order to better match the lithofacies descriptions as given in Chapter 3. 106

Figure 7.6 Well J4930008LK. The detailed representation (A) is from Petrel. It shows both lithofacies lists used, namely the DSL lithofacies in the left column (lithofacies group C) and the reduced lithofacies in the middle column (lithofacies group D). The column to the right shows the result of proportional layering. The DSL profile (B) is again provided as a comparison. 107

Figure 7.7 The proportion of lithofacies present before and after lithofacies modelling. The percentage of a lithofacies present is shown on the y-axis, and the lithofacies are listed on the

x-axis. The red column represents the original 1D lithofacies as provided by the well logs (reduced from the DSL lithofacies); the green represents the lithofacies proportions after up-scaling (the blocked wells); and the blue logs are the proportions (in 3D) after the lithofacies have been modelled in 3D. The aim is for the 3D model lithofacies to honour the 1D input data in 3D. The results, however, show a decrease in structureless sandstone and a proportional increase in structured sandstone. 108

Figure 7.8 The results of the first facies model run, using the Kriging algorithm, and it is immediately evident that too little variation is present (17 lithofaceis were used, yet only 3 are visible). (B) is the cross-section through (A). The purple balls represent well data points. ... 109

Figure 7.9 The facies model using the Sequential Gaussian algorithm. (B) is the cross-section through (A). Note the large variation in lithofacies that can be observed, as opposed to the Kriging model in Fig 5.12. 110

Figure 7.10 The final result. This model was the last to be created. It used the constrained polygon, and the reduced lithofacies. The result was a model that very closely matched the CorelDraw panels. Two cross-sections were created in roughly the same locations as the CorelDraw panels 3 and 12. 111

Figure 7.11 Panels 3 and 12 as seen in the final Petrel facies model. Both are at 10 times vertical exaggeration. The blocked (upscaled) wells are shown to relate the accuracy of the overall results to the original data. Overall, the 3D spatial variation remains accurate close to the blocked wells. Panel 12 only roughly matches the CorelDraw panel, as Petrel can only make a cross-section as a straight line. 112

Figure 7.12 This figure attempts to show the accuracy with which Petrel created the facies model in regards to the up-scaled wells. With enough wells to constrain the algorithms, Petrel can produce accurate and realistic facies models 115

Figure C.1 The first set of Thickness Maps. 151

Figure C.2 The final set of Thickness Maps. 162

Figure D.1 An example correlation panel created in Petrel, showing both the original DSL facies as well as the grain size. Both the well-tops (dashed lines) and the surfaces (dotted lines) created with the Kriging algorithm are included. Note the mess. The well-tops are at the correct levels, whereas the surfaces are literally all over the place. This is what prompted the use of a different algorithm, as the results gained with Kriging simply weren't useful..... 165

Figure D.2 The same correlation as in figure D.1, only this time the surfaces were omited in order to give a clear representation. 166

Figure D.3 Panel 1 - 2 as represented by Petrel. Here the new facies as well as the new Excel data is represented. This view in 2D provides a much clearer picture of what the “new” data achieved by extending “missing” units to the full length of the field area..... 167
Figure D.4 Panel 3 as represented by Petrel..... 167
Figure D.5 Panel 12 as represented by Petrel..... 168

Chapter 1

Introduction

Introduction

1.1 General

Deep-sea submarine fan deposits are characterised in the mid- and distal fan areas by lobes and lobe-sets that are distributive systems, formed by sediment that was bypassed through incisional channels on the proximal fan and slope (web-based reference 1). Prélat *et al*. (in review) described terminal lobes as "distributive systems at the most down-dip depositional positions of terrigenous sediment transported by gravity flows through basin margins".

Analyses of high resolution seismic and side scan sonar data sets from modern systems (Deptuck *et al*., 2008; Machado *et al*., 2004; Wynn *et al*., 2002; Twitchell *et al*., 1992) have provided an understanding of the volumes and geometries of these features. Several studies on terminal lobe deposits have been performed on outcrop analogues. These include the Upper Carboniferous Ross Formation, Western Ireland (Chapin *et al*., 1994; Sullivan *et al*., 2004), the Permian Brushy Canyon Formation, West Texas, USA (Gardner *et al*., 2003), the Permian Skoorsteenberg Formation, South Africa (Johnson *et al*., 2001; Sullivan *et al*., 2004; Hodgson *et al*., 2006), and the Eocene Hecho Group, Northern Spain (Remacha and Fernandez, 2003).

Typically, the detailed features of lobe deposits, such as architecture, lateral and vertical connectivity, element hierarchy, geometry and volume, as well as lithofacies distribution, are often below geophysical seismic survey resolution. For this reason, they are generally referred to as simply as "sheets" (Shanmugam, 2000). This means there is significant uncertainty in exploration and prediction. This lack of quantitative data limits the "robustness" (web-based reference 1) of 3D reservoir models in appraisal and development projects, which are based on only a small number of wells.

Modern deep-marine settings can provide some data for lobes deposited during transgression and high sea level stands, but the data for lowstand periods, which are generally sand-prone, are not available (note that "sand-prone" is not necessarily an indication for a lowstand period; Wynn *et al*., 2002). It is for this reason that good ancient lobe outcrops, of which the Tanqua Fan Complex (TFC) forms an excellent example, are so important for providing large amounts of quantitative data.

The recently completed EU-sponsored NOMAD project provided a well correlated stratigraphic framework within the high-frequency basin floor fan deposits of the Tanqua sub-basin, combining core data from seven research boreholes with outcrop data (Luthi *et al*., 2006; Hodgson *et al*., 2006; web-based reference 1). The University of Liverpool and the Technical University of Delft, in cooperation with the University of Stellenbosch, recently completed a joint research project on the Tanqua fans (Prélat *et al*., in review). This project was called the Lobe project, which aimed to analyse the architecture, dimension and lithofacies character of the lobes within the individual fans from different positions across the fans (web-based reference 1).

The outcrops in the study area are almost completely undeformed, and are easy to access. This makes these submarine fan deposits ideal for study and provide an excellent analogy for hydrocarbon reservoirs in fine-grained, medium-sized turbidite systems (van der Werff and Johnson, 2003).

1.2 Previous work

As exploration and production of hydrocarbons aims for deeper reservoir targets, so interest in ancient deep-marine deposits, and distributive systems in particular, increases. This has led to several research studies being conducted in the Tanqua and Laingsburg sub-basins over the past few decades. Some of the first work conducted in the south-western Karoo sub-basins, namely the Laingsburg and Tanqua sub-basins, was conducted by Wickens in 1976 for the Geological Survey of South Africa. The results of these studies were published as a M.Sc. thesis (Wickens, 1984; 1994).

In conjunction with A.H. Bouma of Louisiana State University, Wickens *et al*. (1990) conducted a full-scale study of the Ecca turbidites for SOEKOR (Pty) Limited (now PetroSA). Several further studies were also conducted in the area, and include Wickens and Bouma (1991a, 1991b), Viljoen and Wickens (1992) and Scott (1997).

The first major European research in the area formed part of a European Union project. Termed the NOMAD project, in was conducted between 2001 and 2004 in the Tanqua submarine system as a Schlumberger Cambridge Research, Statoil, Technical University of

Delft, University of Liverpool and the University of Stellenbosch. The data were collected as DGPS, core and wireline logs for seven research wells, and were published by Hodgson *et al*. (2006). The core and wireline data were further used by Luthi *et al*. (2006) to characterize the stratigraphic evolution of the Tanqua Fan Complex.

The SLOPE project focused on the basin floor, slope and siliciclastic shelf deposits found in the Tanqua and Laingsburg sub-basins (Fans 1 through 4, Fan System 5, and overlying delta deposits of the Tanqua sub-basin). Phase 1 of the SLOPE project focussed on the Tanqua sub-basin. The study provided a structural geological analysis of the basin, the basin margins, the staging area and the sediment routeing system. Studies conducted during the SLOPE project include King (2004), Wild (2004), Van Lente (2004), Wild et al. (2005) and Van der Merwe (2006).

Numerous other workers have also conducted studies in the area (Fildani et al., 2007; van der Merwe, 2003, 2006; van der Werff *et al*., 2003; Johnson *et al*., 2001; Basu and Bouma, 2000; Wickens and Bouma, 2000; Bouma *et al*., 1991).

The most recent study conducted in the area, of which this study forms part, was the Lobe project. This project included detailed studies on both Fan 3 and Fan 4 (Paulissen, 2007). The results of the work done on Fan 3 are currently in review for publication (Prélat *et al*.). The Lobe project was sponsored by several international petroleum companies, namely Chevron, Total, Petrobras, Maersk Oil, Shell, Statoil-Hydro and PetroSA.

1.3 Aims of this study

The study has five main goals:

1. The assessment of the transition from channelised deposits into sheet (lobe) deposits
2. The compilation of high-resolution outcrop maps, detailing the internal architecture, distribution of lithofacies and characteristics of mid Fan 3
3. The incorporation of data collected for the Lobe project north of the Gemsbok River valley
4. The creation of a conceptual depositional model for Fan 3
5. The construction of 3D realisations, or models, from outcrop data using Schlumberger's Petrel, a powerful seismic-to-simulation program.

By using detailed, centimetre-scale measurements and regional observations, several different map-types can be produced. Among these are isopach (equal thickness), 2D lithofacies and architectural element maps. The detailed data gathering also allowed some basic computer modelling through the use of Schlumberger's Petrel. This part was done to determine if the data gathered could be used effectively in computer simulations, and to determine how many steps could be completed toward a static model.

Data were gathered for the Lobe project by researchers from Liverpool University, from the outcrops to the north of the Gemsbok River valley, on the farms Groot Fontein 35, Bosluis Fontein 73, Zoet Meisjies Fontein 75, Los Kop 74 and Klip Fontein 31 (Prélat *et al*. in review). This study focused mostly on data gathered on the outcrops south of the Gemsbok River valley, on the farms Zoet Meisjies Fontein 75 and Rondavel 34, and along the eastern boundary of Los Kop 74 and the western boundary of Kranz Kraal 83.

The Gemsbok River valley creates a gap in the down dip continuity of the Fan 3 outcrops for several kilometres. Detailed fieldwork by researchers from Liverpool University on the outcrops to the north of the study area extended to the eastern end of the valley, joining up with the work completed in this study. The information gained from this study will allow the two outcrop areas to be correlated. From this it should be possible to determine how the more channelised deposits of the mid-fan area in the south grade into sheet deposits down-dip.

The data gathered and conceptual model developed in the Lobe project provide improved solutions for similar situations in ancient subsurface deep-sea fan environments where, e.g. connectivity of sand-bodies, extent of permeability barriers, geometry and volume of sandstone reservoirs, and their stacking patterns are unknown or uncertain. This project aims to add further information to the Lobe project of a more up-dip scenario.

1.4 Geological Setting

1.4.1 Geology of the area

The Tanqua Karoo sub-marine fans form part of the middle to late Permian-aged Ecca Group, which is exposed in the south-western corner of the Karoo Basin, South Africa (Fig. 1.1). The Ecca Group deposits overlie the glaciogenic Dwyka Group, and comprise the Prince Albert Formation (cherty shale beds), the Whitehill Formation (white-weathering, carbonaceous mudstones), the Collingham Formation (fine-grained silt- and sandstones with interbedded ashes), the Tierberg Formation (dark basinal claystone), the Skoorsteenberg Formation (fine-grained, sand-rich submarine-fan deposits), the Kookfontein Formation (slope and shelf-edge deltaic deposits), and the Waterford Formation (Bouma and Wickens 1991; Wickens 1994, Prélat *et al*., in review).

The Tanqua Fan Complex (TFC) constitutes the Skoorsteenberg Formation. It consists of arenaceous fan deposits periodically deposited into the shales of the Tierberg Formation, interpreted by many authors as deep-water deposits (Bouma and Wickens, 1991; Johnson *et al*., 2001).

The TFC comprises four basin-floor fans, namely Fans 1 - 4 (Bouma and Wickens, 1991; Wickens, 1994; Wickens and Bouma, 2000; Johnson *et al*., 2001) and one lower slope to base of slope fan-system (Fan-system 5; van der Merwe, 2006; Hodgson *et al*., 2006). The fan complex is exposed over an area of about 640 km^2 (Johnson *et al*., 2001; Wickens, 1994). The sand-rich fan systems of the Tanqua sub-basin have overall high sandstone to shale ratios and are mostly fine-grained to very fine-grained throughout the entire succession (Johnson *et al*., 2001; Wickens and Bouma, 2000; Wickens, 1994).

The ages of the identified fans are poorly constrained. An age of ca 270 Ma has been derived from the volcanic ash layers in the Collingham Formation (Turner, 1999). An age of 255 Ma has been constrained to the lower Beaufort Group fluvial deposits, based on fossil assemblages (Rubidge *et al*., 1999). This time-span (270 Ma to 255 Ma) encompasses the submarine fan and deltaic deposits of the western Ecca-group. Recent U-Pb single-grain zircon data, presented by Fildani *et al*., (2007), place the ca 255 Ma age in the Tanqua sub-basin between Fans 2 and 3, with the same age in the Laingsburg sub-basin positioned above Fan A. Deposition of the

Collingham Formation is interpreted to have started at ca 275 Ma. The zircons were recovered from six ash beds in the south-western Karoo Basin.

Figure 1.3 is a diagram indicating the extent of the outcrop for Fan 3. Also indicated are the relative locations of depositional features, namely channel complexes, mid-fan and pinch-out. Figure 1.4 shows a simple depositional diagram for a fine-grained turbidite. The two lines show the locations of some of the outcrops of Fan 3 relative to the model, namely the oblique strike section of the Gemsbok River valley (red) and the dip section of the western end of outcrops (green).

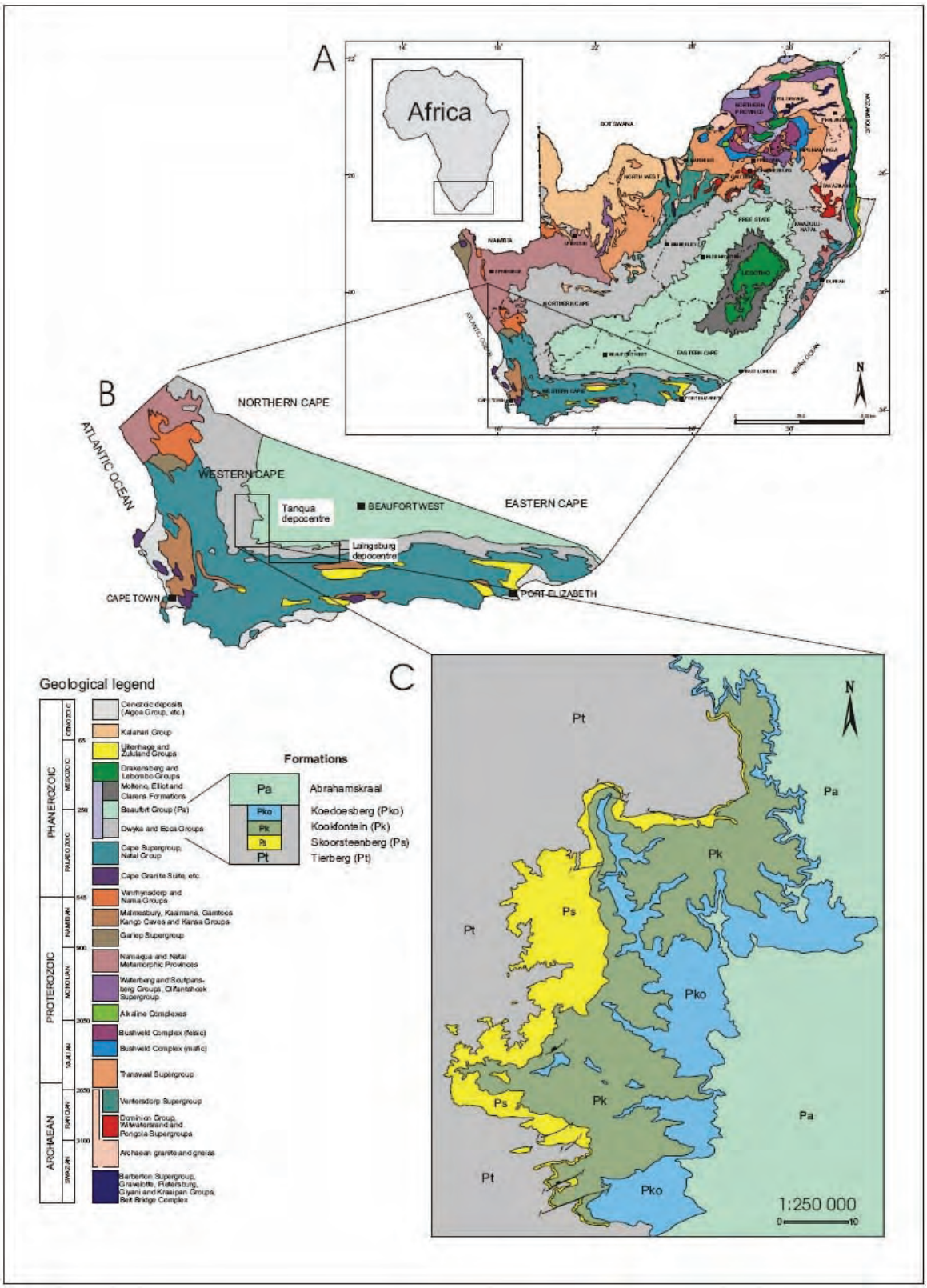

Figure 1.1 A simplified geological map of South Africa to show the location of the Tanqua sub-basin (Geological map, Council for Geoscience, 2000). The Laingsburg and Tanqua sub-basins can be seen in (B). The yellow area in (C) represents the total outcrop of the Skoorsteenberg Formation in the Tanqua sub-basin.

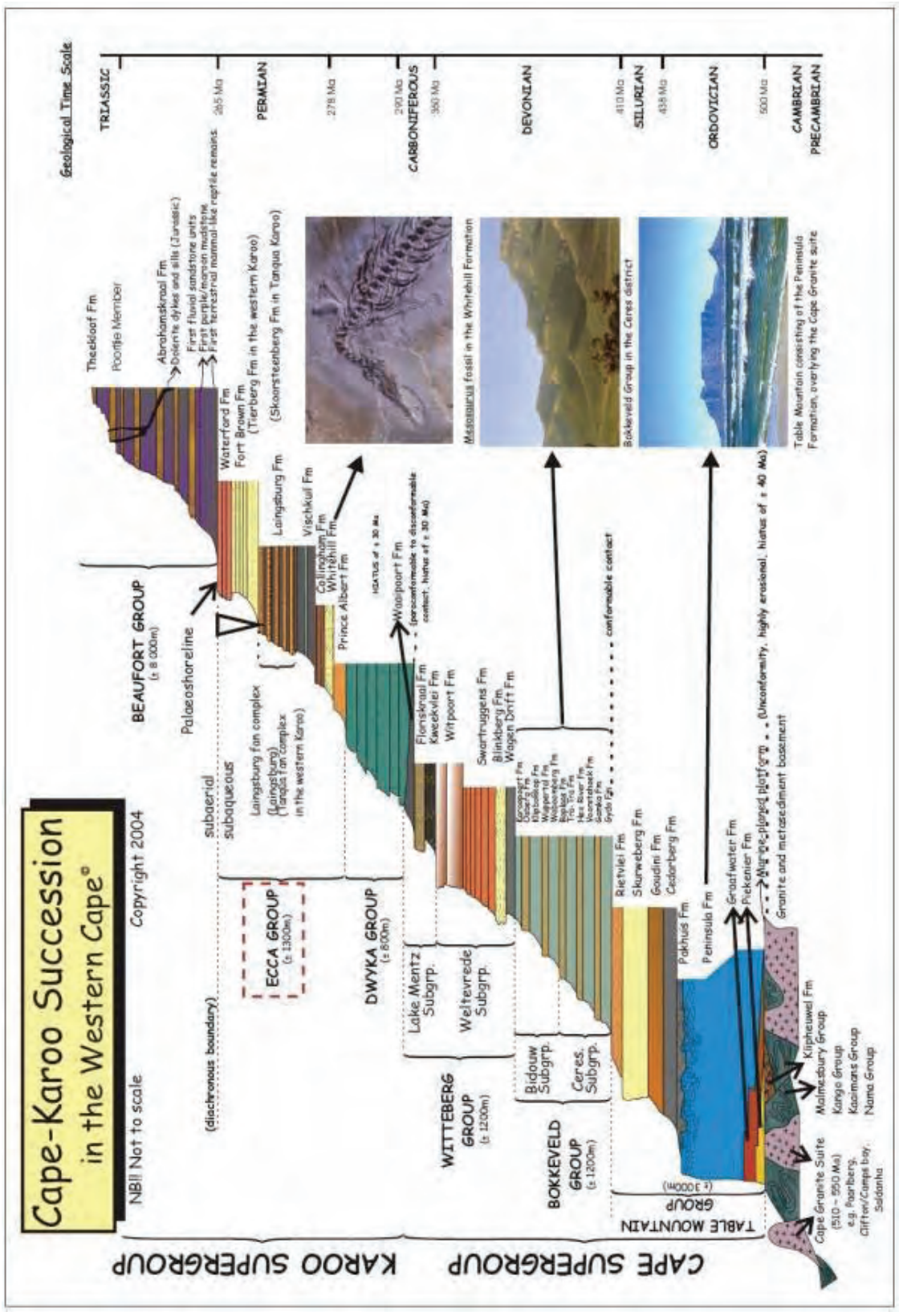

Figure 1.2 A diagram illustrating the location of the Ecca Group in the stratigraphy of the Cape-Karoo Succession (Wickens, 1994)

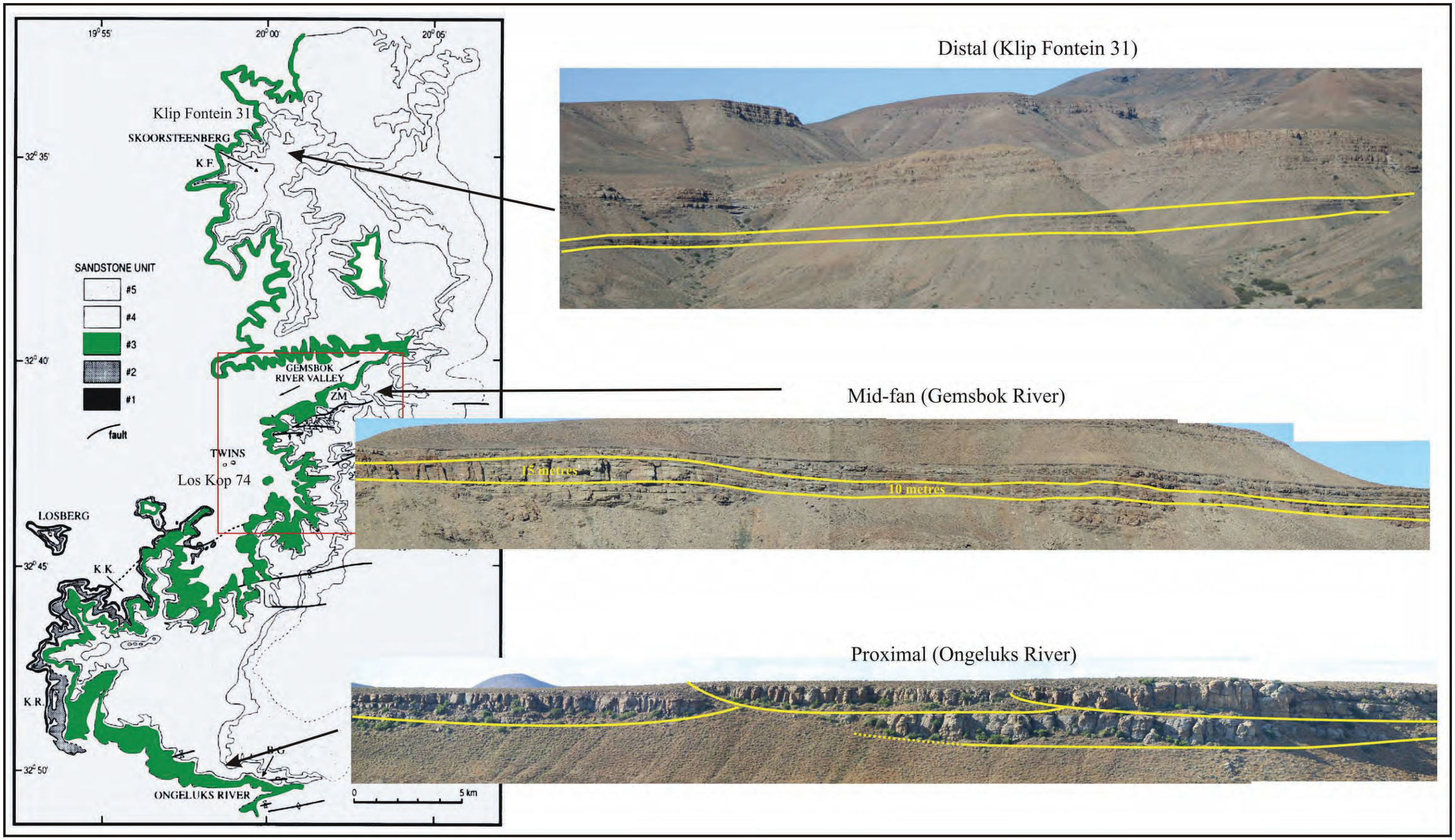

Figure 1.3 Outcrop distribution diagram of the Tanqua Fan Complex with Fan 3 highlighted to show the extent of its outcrop. The red block represents the study area, displayed in figure 1.5. Several panoramic photos have also been added to illustrate the appearance of Fan 3 at selected points of outcrop. Note the stacked channel-fills at the base-of-slope setting at the Ongeluks River. The mid-fan area displays several amalgamated zones, but no true channels. Distal outcrop becomes very thin, with almost no indications of channelised flows. (adapted from Wickens, 1994)

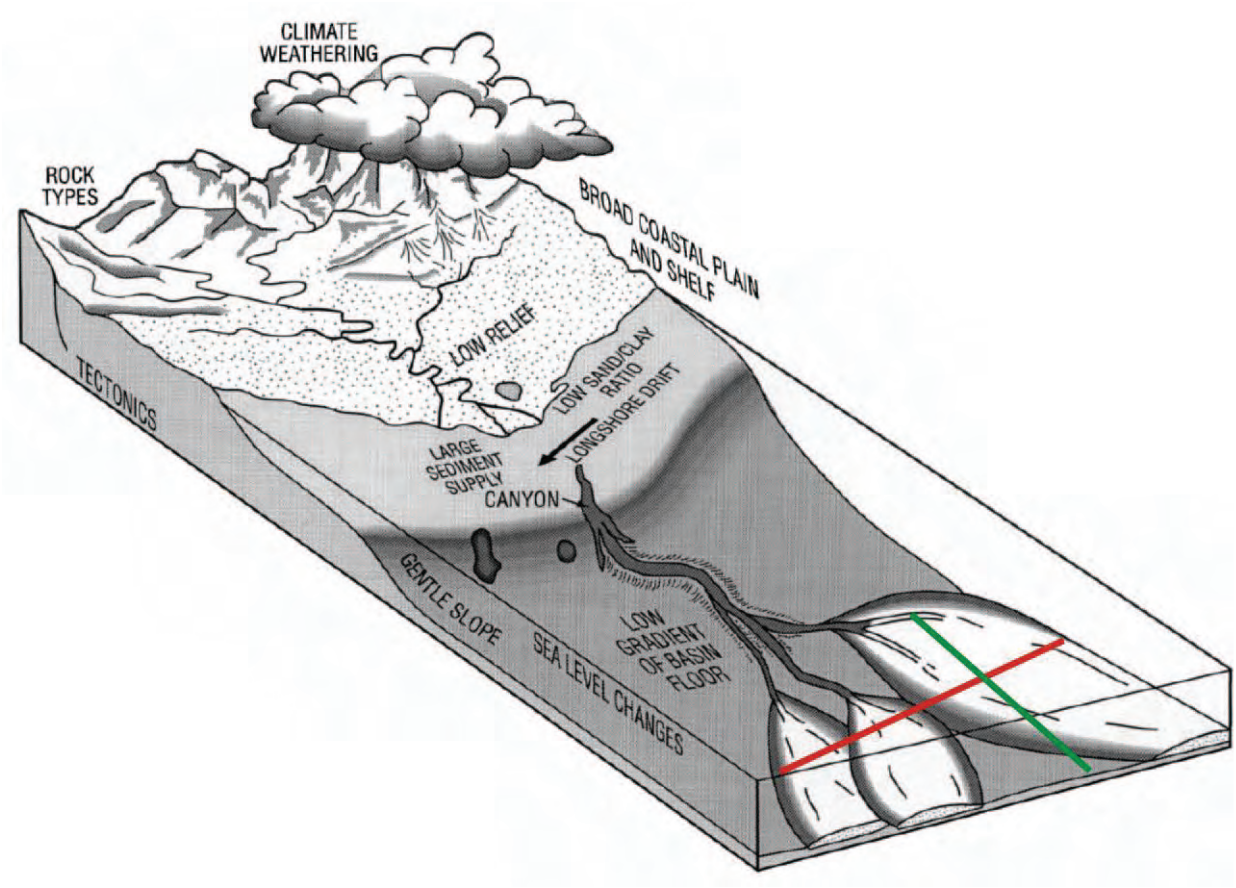

Figure 1.4 Locations of the south Gemsbok River valley outcrops in relation to a depositional diagram for fine-grained turbidites. The red line represents the oblique strike section of the southern Zoet Meisjies Fontein 75 and Rondavel 34 outcrops, and the red line the dip-sections of the Los Kop 74 and Krans Kraal 83 outcrops. Modified from Bouma (2000).

1.5 Methods and Materials

The field area for this study is represented by Figure 1.5. The exposed outcrops represent a 7 kilometre oblique strike-section along the southern Gemsbok River valley, and a 5 kilometre roughly north-south trending dip-section. Several gullies extend westward from this dip-section, providing several shorter up-dip strike-sections.

The outcrops were examined on a centimetre scale by measuring 72 vertical profiles, recording grain-size, bed thicknesses, palaeoflow indicators and other depositional features. Measurements were made using a maximum 1.9 metre retractable Jacob staff and measuring tape. High-resolution digital photographs were also collected of all measured outcrops. Palaeoflow measurements were taken using a Krantz geological compass, with a declination set to 20°.

Some 200 palaeoflow indicators were measured, the majority of which are ripple cross-laminations in plan view, and sole structures. A handheld GPS receiver was used to mark top and base locations of each profile.

The positioning of the profiles was determined mostly by outcrop quality. Along strike, the outcrops are fairly continuous and easy to correlate. Down-dip, the gully strike-sections were a minimum of 500 metres apart, with no outcrop connectivity. This emphasises another factor on profile positioning: connectivity. Where possible, the most complete outcrops were chosen, preferably with at least the basal siltstones present. Where this was not possible, outcrops were chosen that could be easily correlated with the stratigraphy.

Figure 1.6 is a topographical map of the area (adapted from maps created by the South African Chief Directorate of Surveys and Mapping), indicating the locations and names of all 72 vertical profiles measured in the area. The map was generated using ESRI ArcMap 9.1. The profile names consist of four parts, e.g. J-4930-008-LK. They indicate the author, J, the distance to the first measured profile (the first profile is J0000000LK) in metres, e.g. 4930, the GPS bearing to the first profile in degrees, e.g. 008, and the farm on which the profile is located (for quick localization). The farms are **L**os **K**op 74, **Z**oet **M**eisjes Fontein 75, **R**on**d**avel 34, and **K**rantz **K**raal 83. The names were given in order to accurately triangulate the distances between any two

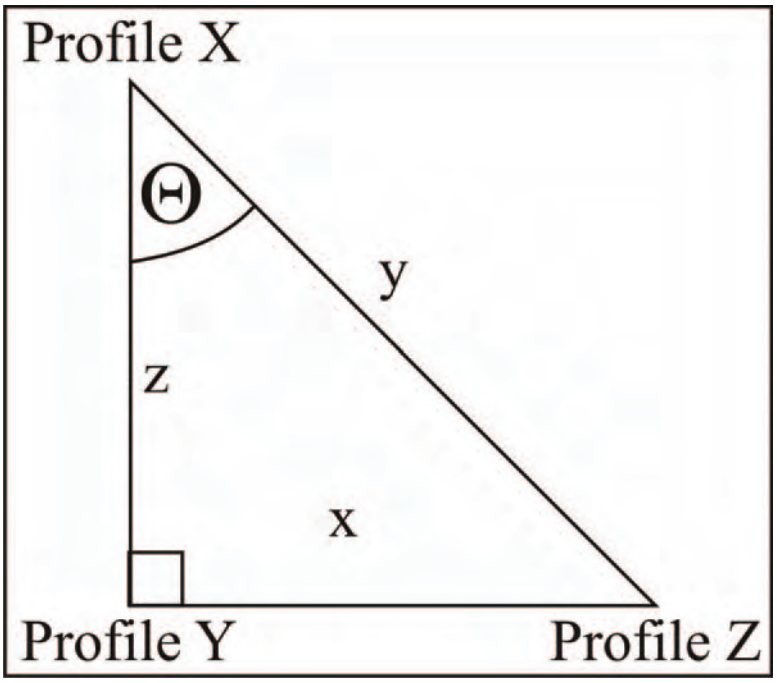

Figure 1.5 Triangle discribing the use of the formula($x^2 = y^2+z^2-2yz\ cos\ \Theta$) to triangulate distances between profiles. x, y and z represent the distances between the profiles.

profiles, using $x^2 = y^2+z^2-2yz\ cos\ \Theta$ (Figure 1.5), and has proven to be a most accurate method.

The vertical profiles were digitised using DSL, an in-house program used by Liverpool University, CorelDraw X3 and Microsoft Excel 2003 (Chapter 5). The CorelDraw profiles were used to create detailed correlation and facies distribution panels. Correlations between profiles were walked out where possible, and determined from a distance using binoculars (easier to get a good lateral overview). The 2D panels were used to describe the stratigraphy and architecture of Fan 3 south of the Gemsbok River valley (Chapter 3). These descriptions, combined with the data from the Lobe project to the north, were used in the construction of a conceptual depositional model for Fan 3 (Chapter 6).

The data were finally manipulated in Petrel (Chapter 7). Petrel was used to create isopach maps, and to create a 3D facies distribution map of Fan 3 south of the Gemsbok River valley. Petrel used the digital data exported from DSL and Excel.

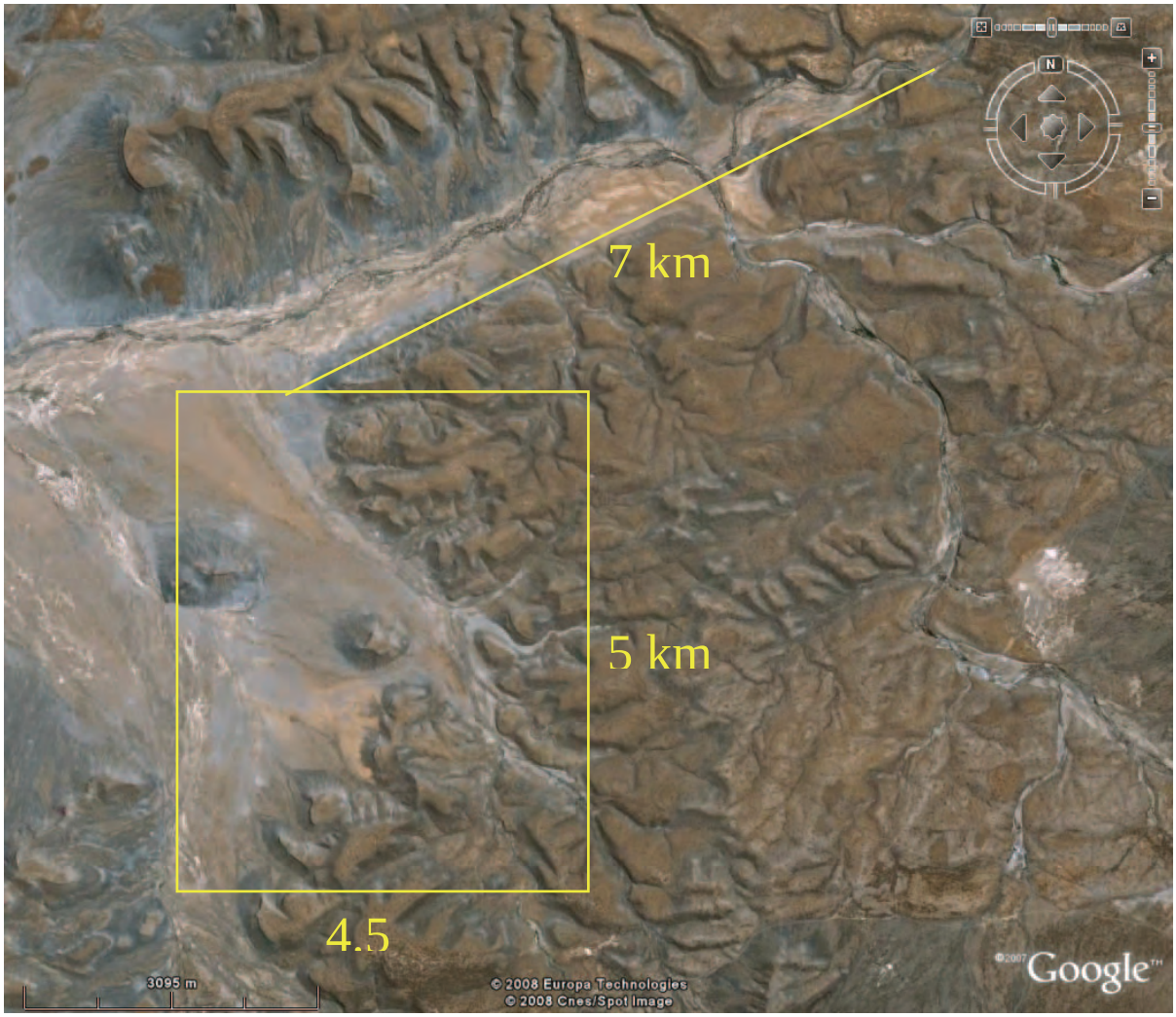

Figure 1.6 Google Earth (2008) satellite image of the study area, indicating the dimensions and location of the field area.

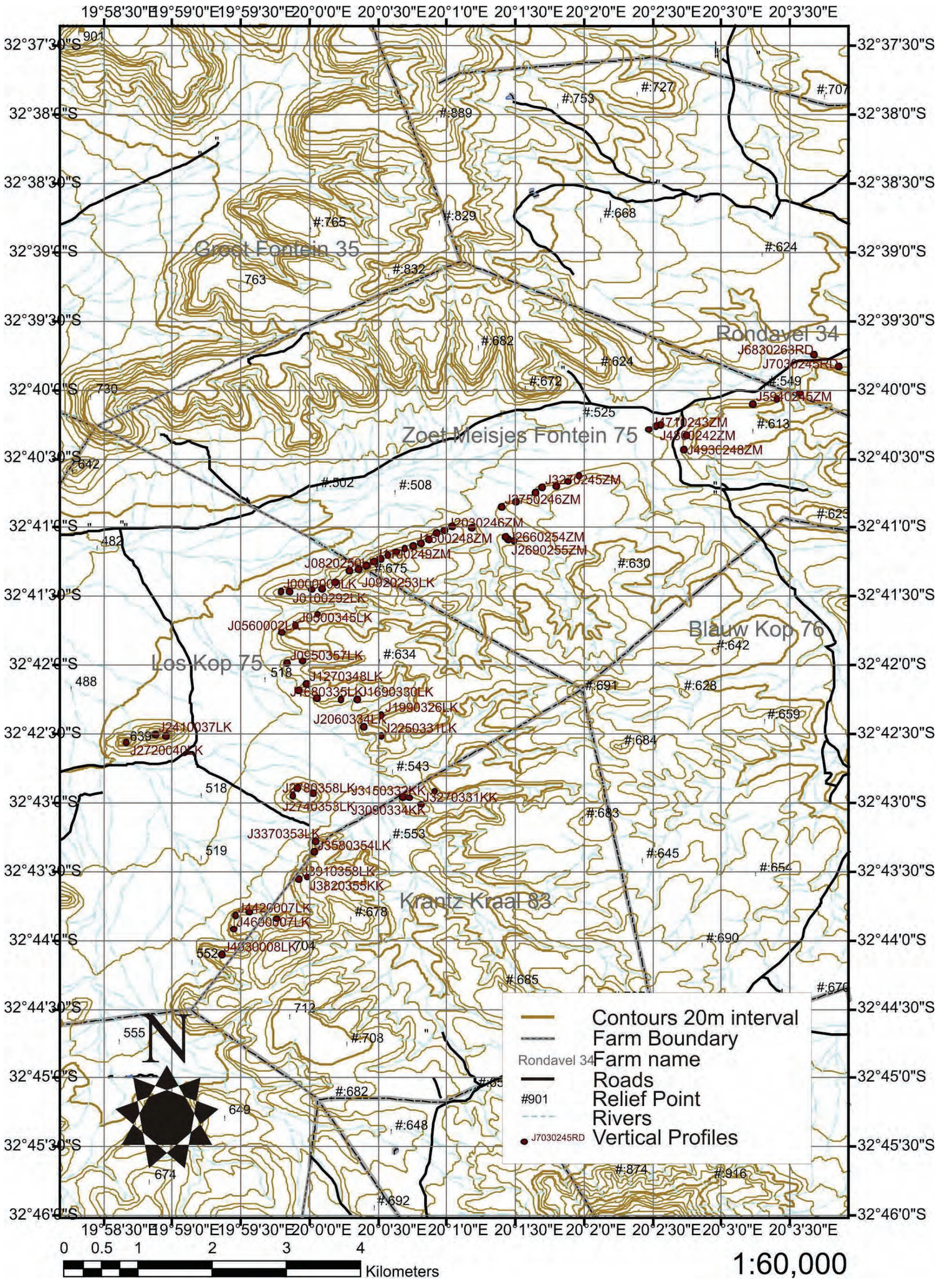

Figure 1.7 Topographic map of the study area. The red dots represent the positions of the measured vertical profiles.

Chapter 2

A brief review of deep-water sedimentation

A brief review of deep-water sedimentation

2.1 Introduction

Research on deep-water sedimentation has been ongoing for several decades. This chapter provides a brief overview of the present knowledge on deep-water sedimentation. The Tanqua Fan Complex is an excellent example of submarine fan deposition, and has been described on several scales of deposition (Wickens and Bouma, 1990; Bouma *et al.*, 1991; Wickens, 1994; Johnson *et al.*, 2001; van der Merwe, 2004, 2006; Hodgson *et al.*, 2006).

The first section of this chapter briefly describes the different types of sediment gravity flows, with particular attention to turbidity flows. Turbidity flows will be discussed in terms of their origins, depositional types and models, and finally their accumulative deep-water depositional features.

2.2 Sediment gravity flow

The term “sediment gravity flow” was introduced by Middleton and Hampton (1973, 1976), and is a generalised term used to broadly describe major flow types that occur under the influence of gravity, found during sedimentation processes. Several different types can be distinguished based on their rheological behaviour. These include slides, debris flows, grain flows, turbidity flows, and liquefied flows. The only flow types that display Newtonian fluid characteristics are turbidity flows and liquefied flows. Debris and grain flows display Bingham plastic flow characteristics (Johnson, 1970; Nardin *et al*., 1979; Shanmugam, 1997).

2.2.1 Slides and slumps

Slides are not strictly sediment gravity flows, as they display elasticity without true grain flow. Slides form due to shear failure along discrete surfaces, and display little to no internal deformation (Boggs, 2001).

2.2.2 Debris flows

An important distinction must be made between turbidity and debris flows: debris flows exhibit strength and the flow is laminar, in other words they do not show fluid mixing across streamlines (Shanmugam, 1997). They are matrix supported, as opposed to turbulence as support mechanism in turbidity flows, and are usually not erosive, a feature attributed to hydroplaning. Hydroplaning causes the basal contacts of massive sandstones deposited by debris flows to be sheared surfaces with inverse grading and poor sorting. Unlike slides, shear is distributed throughout the sediment mass (Boggs, 2001).

2.2.3 Grain flows

Grain flows represent the plastic-liquid flow transition. They generally require a relatively steep slope. Sediment is supported by dispersive pressures such as collisions between grains. It forms a cohesionless mass capable of flow in the inertial or viscous flow regimes (Boggs, 2001).

2.2.4 Liquefied flows

Liquefied flow occurs when a loosely packed sediment structure collapses. Sediment is supported by the upward movement of pore fluid, either through upward escape or injection from below. Flow can only continue as long as grain dispersion is maintained (Boggs, 2001).

2.2.5 Turbidity flows

The definition for a “turbidity flow”, or “turbidity current”, has remained fairly constant over the last few decades (Shanmugam, 1997). Shanmugam (2000) describes a turbidity current as a sediment gravity flow with fluidal Newtonian rheology and turbulent state from which deposition occurs through suspension settling. They form due to density contrasts between the flow and the ambient water, and are not simply non-uniform waning flows (Kneller 1995). Turbidity flows can be caused by several mechanisms, including sediment failure and sediment

flow caused by surface events, such as storms, and denser bedload inflow from rivers, creating hyperpycnal flows (Boggs, 2001).

2.3 Deposits of turbidity flows

2.3.1 Introduction

A turbidity flow can be divided into three parts, namely the head, the body, and the tail. These were first described by Middleton (1966, 1967) in gravity surge experiments. The focus of the turbidity flow is located in the head, with the body already displaying a steady current. The tail is simply the dilute part dragged behind the main flow.

2.3.2 Deposits formed by turbidity flows

A distinction is generally made between high-density and low-density flows (Lowe, 1982). High-density flows are characterised by coarse-grained and thick-bedded deposits generally displaying poor grading, with little to no basal scour features. Low-density flows on the other hand tend to form thin-bedded and fine-grained deposits displaying laminations and grading, as well as basal scour features.

Deptuck *et al*. (2008) indicate several controls influencing the deposits formed by turbidity currents. These are: flow properties (volume, velocity, duration, grain-size and concentration); the frequency of flows as well as their temporal variation; gradient change and the morphology of the sea floor at the feeder conduit; the life-span of the lobe prior to avulsion and abandonment; and the geometry and stability of the feeder channel. It was shown that, in general, lobes (or even fans) outboard of stable fan valleys tend to form longer, wider and thicker deposits in more basinal environments, provided they are still connected to shelf-incised canyons.

2.3.3 Models of turbidite deposition

In his 1962 publication *Sedimentology of some Flysch deposits: a graphic approach to facies interpretation*, Bouma introduced a simple and useful technique for classifying the internal

architecture of idealised turbidites. It has become one of the most used techniques for describing turbidites, both in outcrop and subsurface (Shanmugam, 1997; Miall, 1995). Although there has been refinement over the years, the general pattern has remained the same. It is especially useful for quick classification where not much detail is required.

The Bouma sequence consists of a series labelled Ta to Te. Ta represents the large, structureless sandstone units deposited in the upper flow regime. They typically show normal grading due to good sorting by the depositing turbidity current. Tb is parallel laminated sandstone. The flow strength is somewhat reduced from Ta, but not enough to produce ripples. Tc is the ripple cross-laminated sandstones, deposited during significantly reduced flow. They are particularly common away from areas of focussed flow. Td units are parallel laminated, fine-grained units, representing starvation of the turbidity flows. The last unit is Te, and represents the deposits formed during the weakest flow. They may represent hemipelagic claystones, and therefore do not necessarily form part of turbidity deposits (Boggs, 2001).

However, the Bouma sequence represents a simplification of complicated features (Shanmugam, 1997), and all five divisions are rarely found in a single turbidite deposit (bed). Stow and Shanmugam (1980) proposed an eight-fold classification as a refinement of the Bouma sequence, although this only provides more detail for the Bouma Tc to Te subdivisions. The Bouma Ta and Tb subdivisions are unchanged. Both of these classifications are used for low-density flows. For high-density flows, the Bouma Ta subdivision can be detailed by Lowe's (1982) divisions, with a few extra divisions added to the base.

While all three divisions (Lowe, 1982; Bouma, 1962; Stow and Shanmugam, 1980; Fig. 2.1) are useful, they can easily be misinterpreted or wrongly applied (Shanmugam, 1997a). Also, it is possible for a turbidity current to possess the full range of grain sizes, from gravel to mud, which allows it to form deposits representing both debris flow and turbidity currents. Shanmugam (2000) therefore suggested a combined sequence. Again, this sequence of 16 divisions has never been documented, and only represents an idealised model.

It should be noted that grain-sizes of the TFC never exceed fine-grained sands. Therefore the Lowe subdivisions (R1 – R3 and S1 – S3) are not applicable.

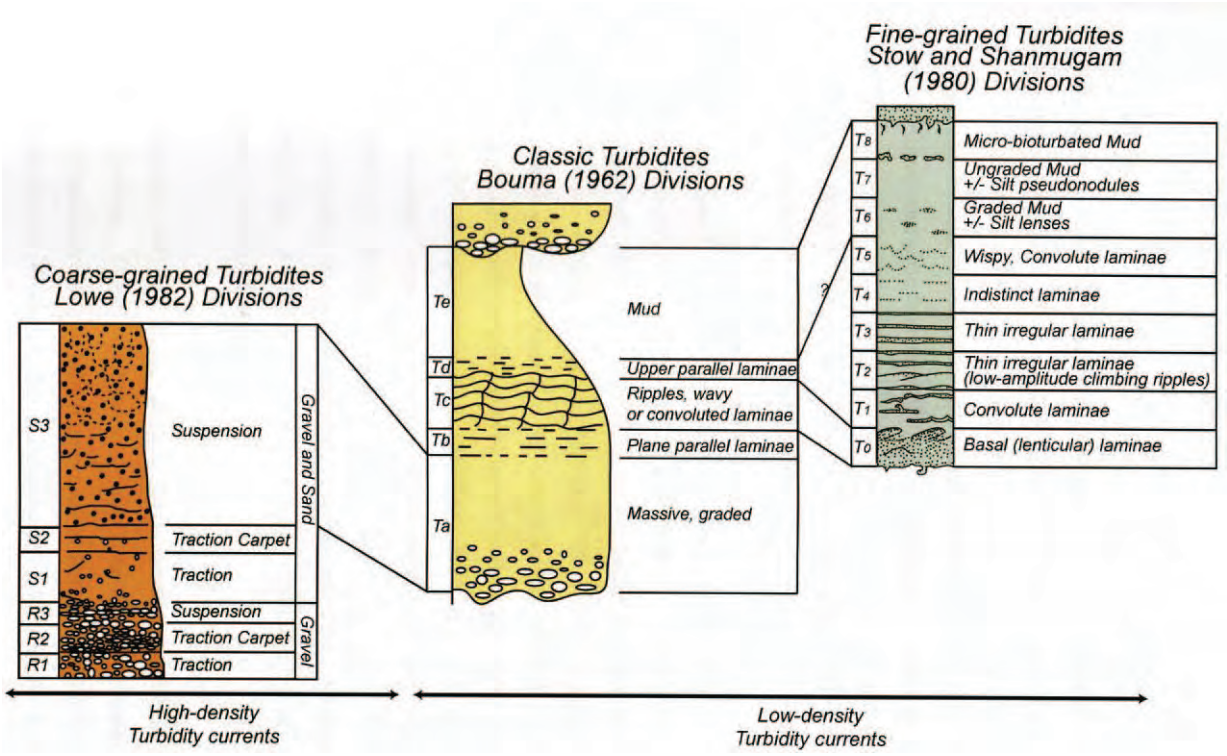

Figure 2.1 A summary diagram of the Lowe (1982), Bouma (1962) and Stow and Shanmugam (1980) subdivisions for turbidites (from Shanmugam, 2000).

2.4 Terminology

A hierarchical subdivision is used in order to compare the different stratigraphic and architectural elements. The mid- to outer part of Fan 3 can be subdivided into several lobes, each of which consists of one or more lobe-elements. A lobe is defined in the Lobe project as a set of lobe-elements, be they amalgamated or bedded, separated from other lobes by significant thin-bedded, fine-grained siltstone breaks that can be traced along strike and dip for several kilometres. The above terms can be compared with a hierarchical classification provided by Mutti and Normark, 1987, to provide a rough estimate of the time constraints involved during the formation of turbidites. For example, their "Turbidite system" conpares with "Lobe-complex" in the Lobe project, whereas their "Turbidite stage" compare to "Lobe".

Chapter 3

Sedimentology, Stratigraphy and Architecture of Fan 3

Sedimentology, Stratigraphy and Architecture of Fan 3

3.1 Geology of Fan 3

Fan 3 is exposed over a distance of 34 kilometres from the Ongeluks River in the south, to its pinch-out just north of the farm Klip Fontein (Fig. 1.3). The outcrops of Fan 3 represent base-of-slope to pinch-out. It is separated from Fan 2 by 50 metres of hemipelagic shales, with occasional siltstone and thin sandstone beds (Wickens *et al*., 1990). The fan itself varies in thickness from 30 to 50 metres in the more proximal areas to the south, and gradually thins towards the north.

Of all the fans in the Tanqua sub-basin, Fan 3 is considered to be the most complete (Wickens and Bouma, 2000). Because of this, it has the largest variety of lithofacies and architectural elements. Discreet channel-fill complexes and complex-sets are present in the most proximal parts of the fan (Hodgson *et al.*, 2006), with levee-deposits and transitional channelised to non-channelised deposits in the mid-fan area, stacked sheet-sands in the north, and overbank deposits along the western margin of the fan (Wickens and Bouma, 2000).

3.2 Lithofacies

3.2.1 Lithofacies 1: Claystone

Description:

Generally, claystones (commonly referred to as shale) are horizontally laminated, but appear structureless due to their fine-grained nature. At outcrop, the claystones all display flaky, pencil-like weathering, and have a blackish colour. The claystones are present above and below some of the more complete measured sections. They represent all rocks with a grain-size of 0.004mm or less. The upper and lower contacts of the fan are generally sharp. The claystones commonly contain concretionary horizons.

In some locations, the break between the shale and the first siltstones is ambiguous. In these cases the claystones gradually grade into siltstone, without a distinct break. The distinction between the two is the greenish weathering of the siltstone (Hodgson, personal communication),

as apposed to the darker colour of the claystones, as well as the bedding pattern of the siltstones. Siltstones generally display a laminated nature, be it parallel- or ripple-laminated, whereas the laminations of claystones are usually not easy to discern.

Interpretation:

The claystones are interpreted as the result of background suspension sedimentation taking place continuously in the basin. The siltstones are interpreted as low-volume, low-density turbidites. The transitional base and top of the fans respectively mark the initiation and decay of the fans (Hodgson *et al.,* 2006). The true stratigraphic base and top of the fan is rarely identified at outcrop, but is clearly seen in well logs (Luthi *et al.*, 2006) and core (Hodgson *et al.*, 2006) from the research boreholes.

3.2.2 Lithofacies 2: Parallel- and ripple cross–laminated siltstone

Description:

These fine- to very fine-grained siltstone units are mostly finely laminated to micro-cross-

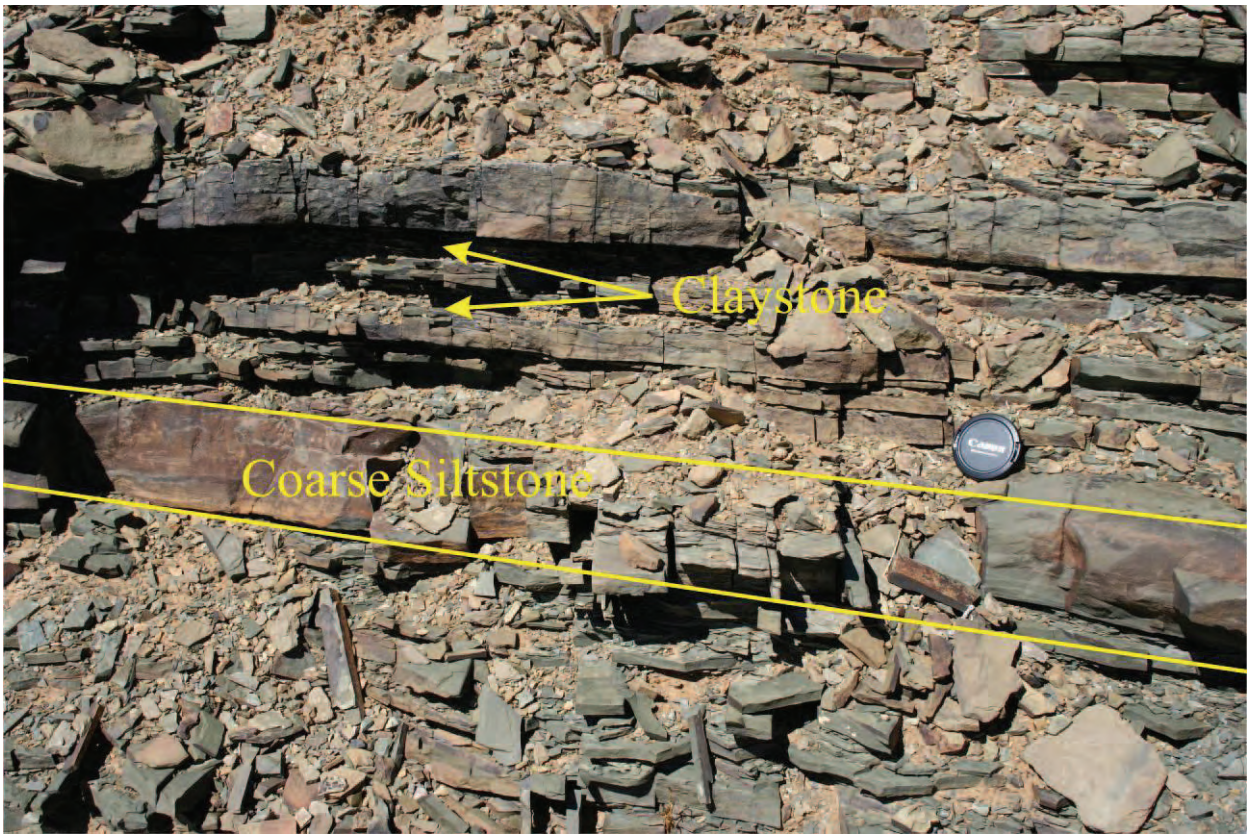

Figure 3.1 An example of the siltstone to claystone relation close to the base of the succession. This relation is only present at the base and top of Fan 3, as no claystones are present within the fan succession.

laminated, and are commonly interbedded with layers of very fine-grained sandstone or claystone of a few centimetres in thickness (claystone is only present close to the lithological base of the fan; Fig. 3.1). The sandy units (beds) tend to thicken upwards in the succession, whilst the siltstone units thin to millimetre scale units. The reverse holds true for the top of the succession. The siltstone successions generally form the breaks between the individual lobe elements of Fan 3. This lithofacies can also be treated as a lithofacies association: Johnson *et al.* (2001) refer to this grouping of siltstone grading into sandstone as thin-bedded turbidites.

In cases where the siltstones form breaks between the sandstone units (lobes), they form a fairly distinct alternating pattern (Fig. 3.2). They consist of alternating fine- and coarse-grained siltstone units, and individual units vary greatly in thickness, as do the successions. The former varies between a few millimetres to almost 30cm, and the latter can be anything from less than 5cm to almost 2 metres. There is no perceivable pattern along strike as to the exact thickness of

Figure 3.2 Alternating relationship between coarse- and fine-grained siltstone that is present throughout the study area. This relationship forms the most common breaks between lobes. They are commonly referred to simply as thin-bedded intervals.

individual units. Down-dip from the Gemsbok River valley, these siltstone successions become slightly thicker, and in some cases begin to either grade into, or are interbedded with very fine-grained, thin-bedded sandstone units.

There are also several thinner, but by no means less extensive, siltstone units interbedded within individual sandstone lobes. These are mostly extensive enough to be traced along strike and down-dip for several kilometres. For this reason they are used to subdivide lobes into smaller lobe-elements. These thinner siltstones are also the first units to disappear when sandstones thicken and amalgamate, making them somewhat difficult to trace in instances where amalgamation continues for several hundred metres.

Aside from the examples mentioned above, there are also numerous thinner and less extensive siltstone units located throughout the lobes. These are usually confined to the more bedded areas of the lobes, away from channelised locations.

Interpretation:

These siltstone packages result from diluted, low-density turbidity currents and represent the Bouma Td successions. The reason for this is the fact that they are very-fine grained, possibly representing abandonment, and display lamination.

There is the possibility that the thicker, coarser-grained siltstone units represent very fine-grained, low-volume turbidites. In these cases they would represent Bouma Tb or Tc successions, depending on the laminations present.

3.2.3 Lithofacies 3: Structureless sandstone

Description:

Structureless sandstones are easily the most recognisable features in these outcrops (Fig. 3.3). They are thick, i.e. more than 1 metre, and at outcrop are structureless (Stow and Johansson, 2000). These units will be referred to as *structureless sandstone*, and not massive sandstone, as massive can be confused with size.

Figure 3.3 An example of the general appearance of structureless sands in the study area. This particular section is located in one of several highly amalgamated channelised areas, with sandstone cliffs reaching 10 metres or more in thickness. Note person for scale underneath the overhang (circle).

Amalgamation of individual sandstone units is common. The contacts with other lithofacies are generally sharp and planar. Irregularities such as those caused by loading and local scouring are also common. Rip-up clasts of finer, softer lithologies (claystones) are commonly associated

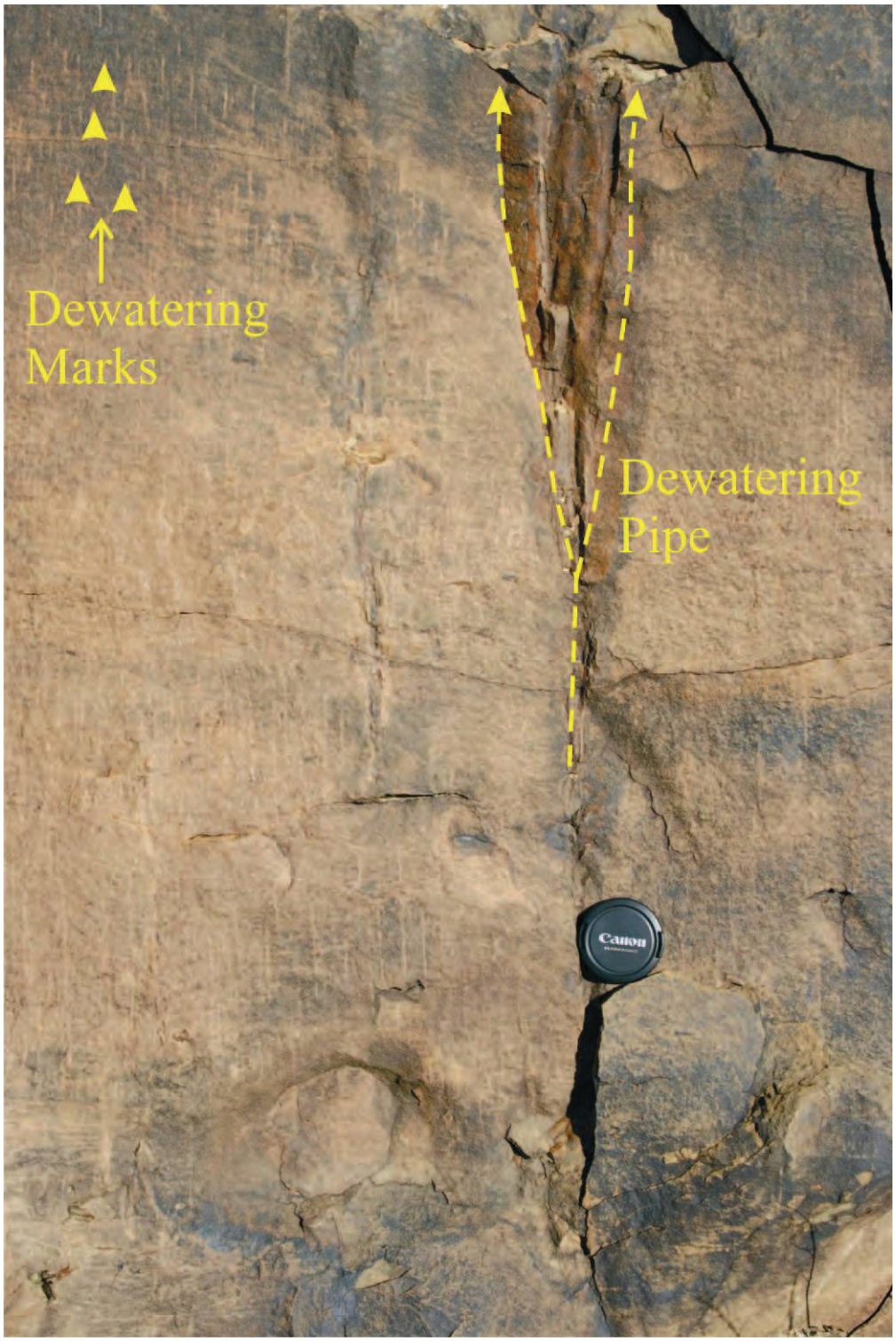

Figure 3.4 Example of the dewatering features found in structureless sands. Here the smaller linear features are present, as well as a much larger dewatering pipe with significant alteration along its edges.

with the amalgamated surfaces. They are common lower down in the succession, associated with the earlier sandstone units. Clasts are generally angular and elongated. Clast-rich units become more prominent higher in the stratigraphy and closer to the margin of the fan, as lower stratigraphic units slowly pinch out.

Several elongated and/or rounded calcareous concretions of various sizes (up to 1 m in diameter) are also present near to the base of some of the thicker sandstone units (Fig. 3.7).

Interpretation:

Structureless sandstones represent the Ta units in the Bouma subdivision. Dewatering features (mostly at the top of the succession in the study area; Fig. 3.4), deformation of the lower contacts (Fig. 3.5), rip-up clasts (Fig 3.6), amalgamation of beds and sole structures can all be used to infer the velocity and density of currents, as well as the transport mechanism active during deposition of the sediment. Clasts are especially common in high-energy channelised environments, whereas sole structures are generally at the base of thicker sandstone units.

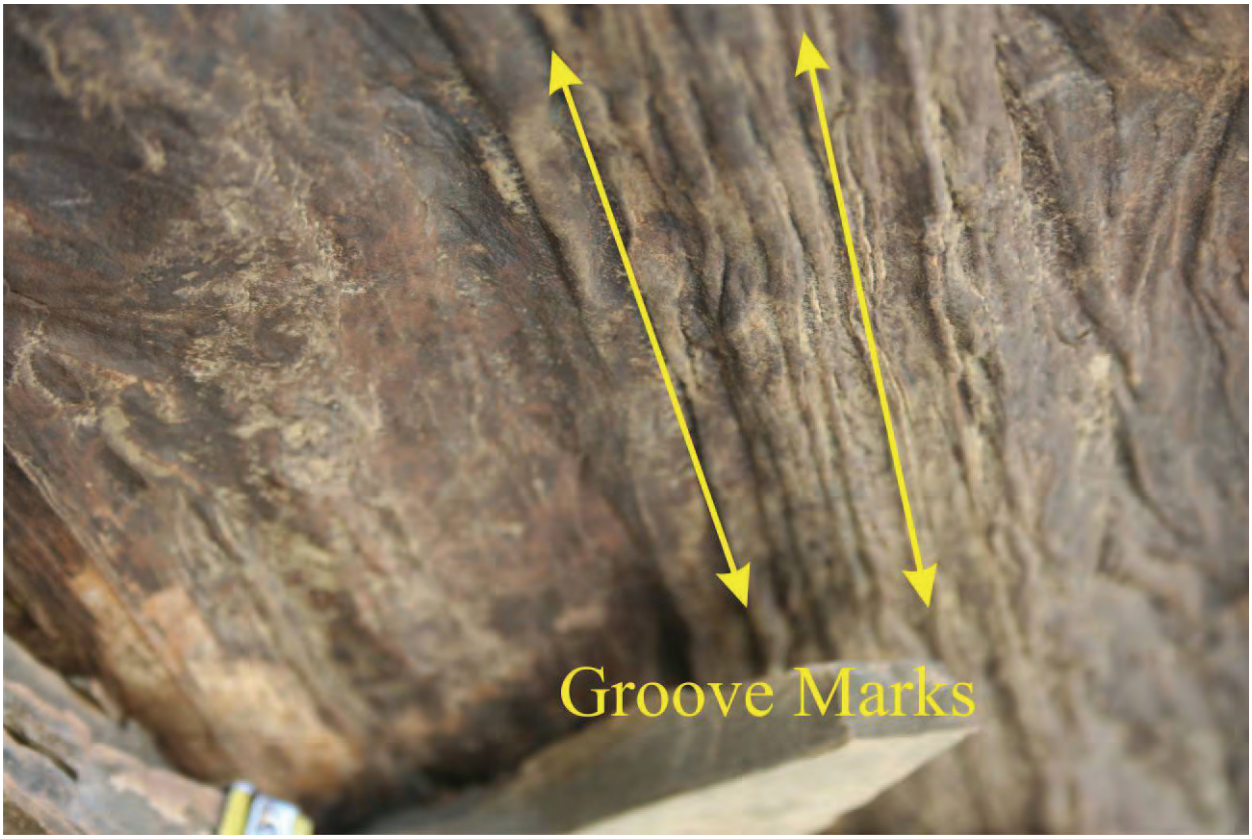

Figure 3.5 Groove marks at the base of a structureless sandstone. These marks infer the general orientation of palaeocurrents.

Figure 3.6 Example of a rip-up clast near the base of a thick sandstone unit. This example is near the base of Fan 3, close to the eastern margin of the fan.

Figure 3.7 An example of a particularly large calcareous concretion. Note the concentric growth pattern.

3.2.4 Lithofacies 4: Structured sandstone

Description:

Structured sandstone contains either parallel- or ripple cross-lamination features. Generally these are easily distinguished from structureless sands, but in some cases the latter grades into structured sandstone (Fig. 3.8). Where no clear-cut break could be distinguished between structureless and structured sandstones, the lithofacies was classified as structured sandstone. Wherever the sandstone packages become more stratified, i.e. away from amalgamated or channelised areas, they are referred to as structured sandstone. These beds also tend to show a greater number of sedimentary features.

Where breaks can be clearly distinguished, the lithofacies can be either parallel- or ripple cross-laminated sandstone (Fig. 3.10). The bed thicknesses of these layers vary greatly. They are

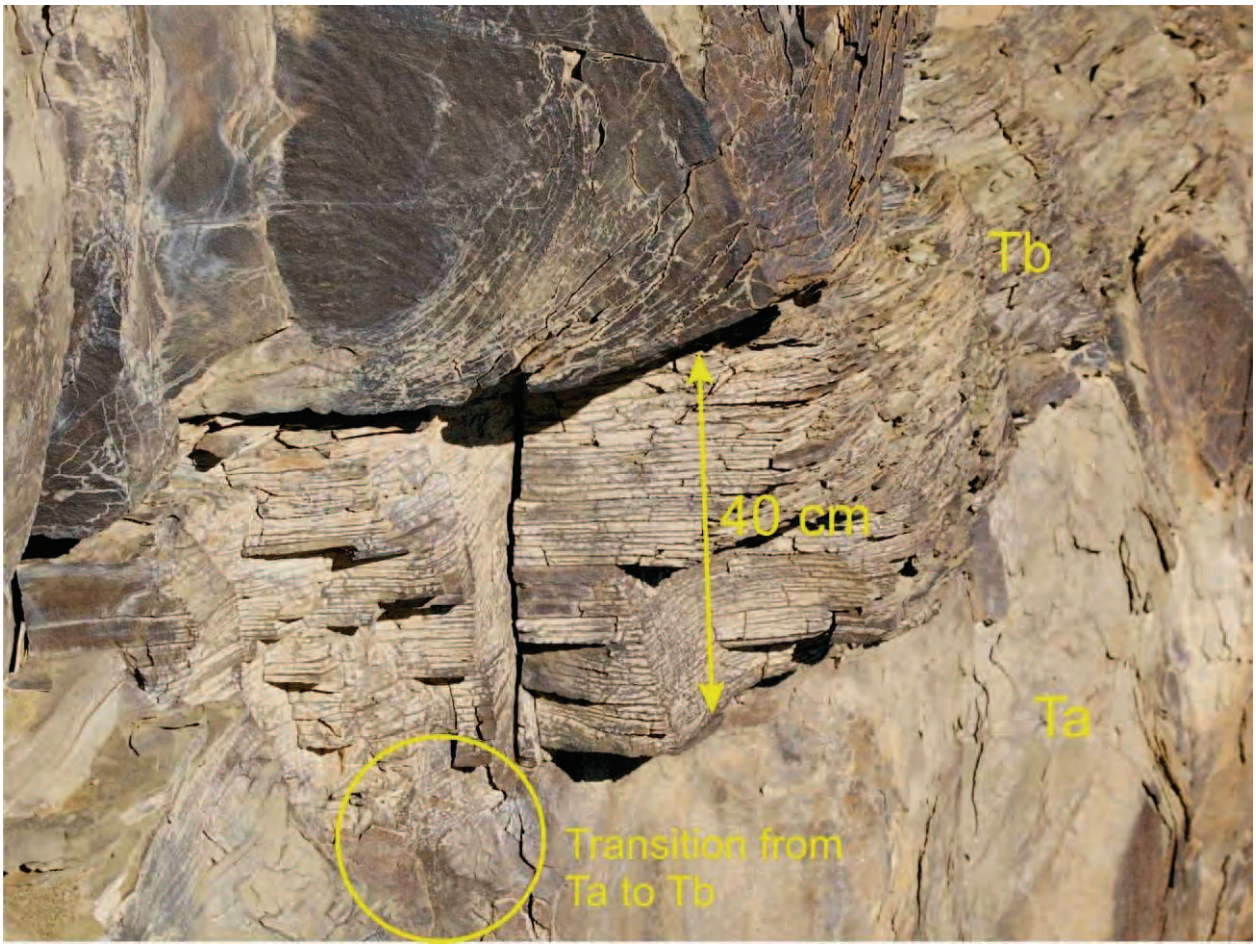

Figure 3.8 An example of where the transition between Ta and Tb is not particularly clear-cut. The transition only becomes apparent laterally. This particular feature is fairly common along the Gemsbok River outcrop.

generally much thinner than structureless sandstones, with grain sizes varying from fine- to very fine-grained sand. The parallel-laminated sandstone beds of this lithofacies mostly overlie the structureless sandstone units. Parallel-laminated sandstones occur throughout most of the study area to a greater or lesser degree, and are especially common close to channelised areas (structureless sandstones become more bedded away from channelised areas). They are especially common closer to the margin of lobes, far away from areas of focussed flow and in overbank deposits.

Interpretation:

Parallel-laminated sandstones represent deposition in the upper flow regime, representing the Bouma Tb division. Ripple cross-laminated sandstone represents the Bouma Tc division, and generally overlay the parallel-laminated sandstones (Fig. 3.9). Structured sandstone commonly forms thicker successions away from channelised areas, the latter being dominated by structureless sandstones.

Figure 3.9 An example of the sharp transition between a Tb and Tc succession.

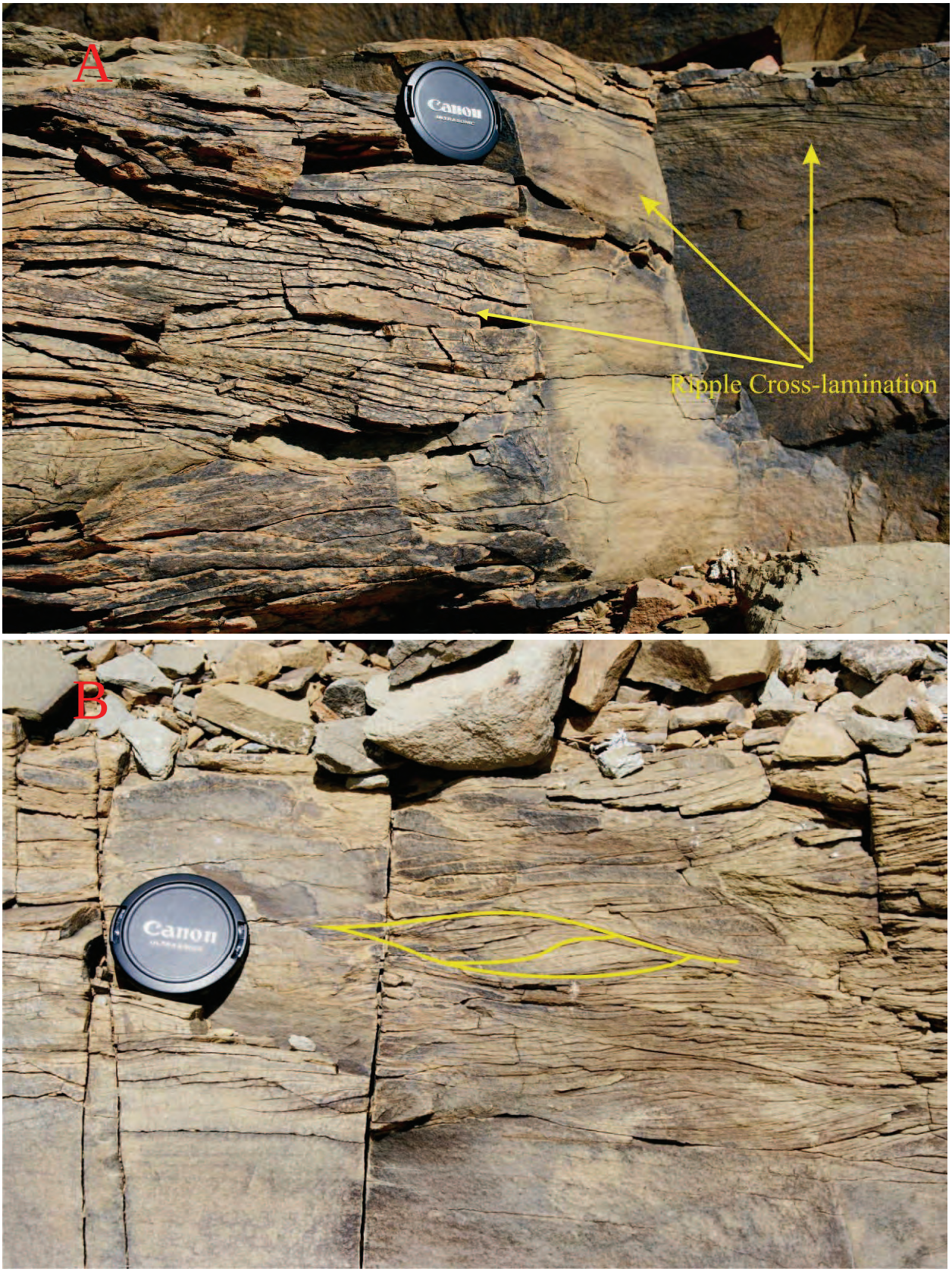

Figure 3.10 Closer views of ripple cross-laminated sandstone: (A) Ripple cross-lamination; (B) Climbing ripple-lamination.

3.2.5 Lithofacies 5: Mud-clast conglomerates

Description:

The term “mud-clast conglomerate (MCC)” is a collective term used to describe a “nest” of rip-up clasts in a matrix of either sand or silt. The clasts generally appear as a collection of small (less than 5 cm) elongated slivers of mud. MCCs can be found either above or below thick sand units. They often resemble lag deposits when found below the base of sandstone beds (Fig. 3.11). All of these deposits have in common the lack of internal structure.

Interpretation:

MCCs commonly form in the thalwegs of channels as a result of bypassing of high-energy flows. Clay clasts can originate during erosive undercutting and by local rip-up by strong, high-density turbidity currents. Lag deposits, as well as debrites (MCCs with large amounts of organic material), represent the final trailing of sediment or debris pulled behind the turbidity flow. The turbulent nature of the flow ensures these are the last components to be deposited, often close to the margin of a lobe.

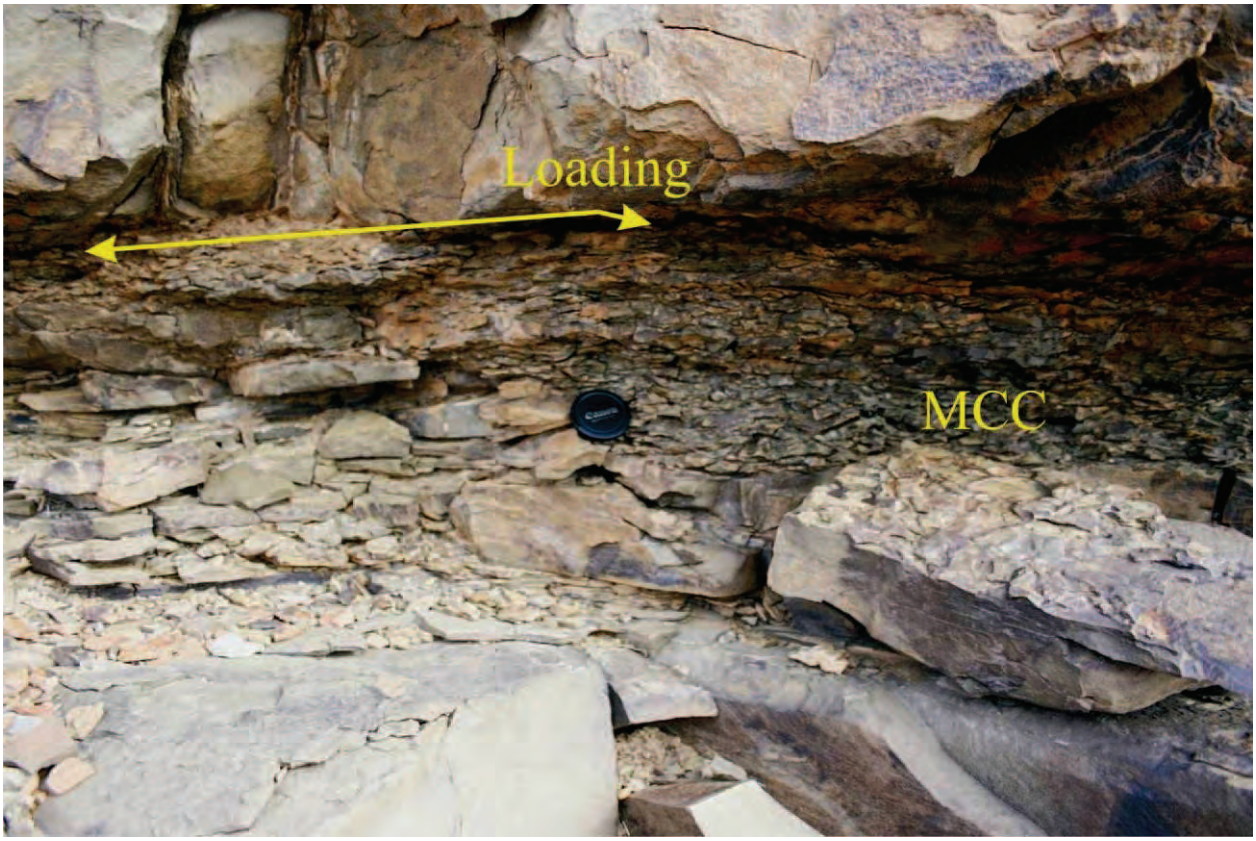

Figure 3.11 This is how mud-clast conglomerates mostly appear in the study area. This example lies at the base of a large structureless sand, the latter loading into the MCC.

3.3 Stratigraphy

3.3.1 Introduction

Mid- to lower Fan 3 can be subdivided into several lobes, each of which consists of one or more lobe-elements. Figure 3.12 shows the subdivision as defined in the Lobe project.

A fan is built up by a series of stacked lithological units: The initial beds and bed-sets ("bulb" deposits as described by Machado *et al.*, 2004); lobe-elements, singular discrete sedimentary units consisting of stacked beds (Deptuck *et al.*, 2008); lobes, which are separated by significant thin-bedded, fine-grained intervals (referred to as *composite lobes* by Deptuck *et al.*, 2008); and a lobe complex, or fan (Fig. 3.12). Importantly, a lobe complex will thin to a lobe, and a lobe will thin to a lobe-element, and a lobe-element will thin to an individual bed.

Six lobes have been identified to the north of the Gemsbok River (Prélat *et al.*, in review). Most of these are traceable to the northern pinch-out of Fan 3. Of these six lobes, only five are present south of the Gemsbok River. The missing lobe, Lobe 3, is rarely more than a single bed

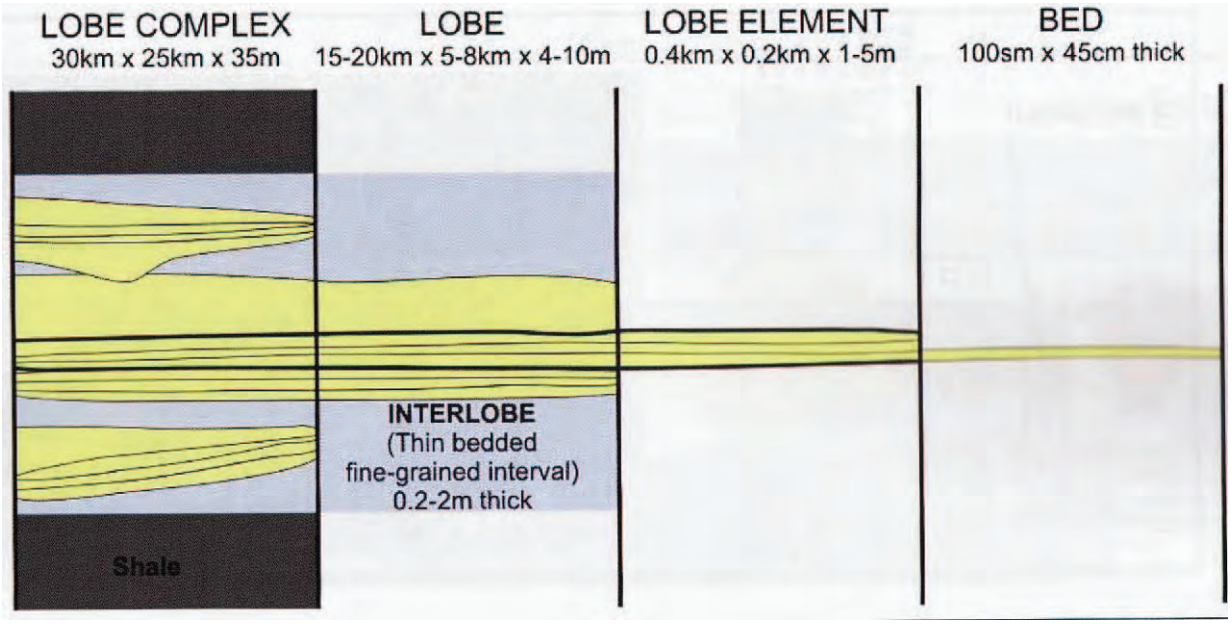

Figure 3.12 Hierarchy of depositional elements in distributive deep-water systems. The division consists of four scales of elements, namely single beds, lobe-elements, lobes and the lobe complex (or fan) defined by the bounding fine-grained units and mappable extent, not thickness. Lobes are separated by interlobe units of fine-grained, thin-bedded siltstones (From Lobe Field Guide, © STRAT Group, University of Liverpool, June 2008).

to the north. However, two additional lobes were identified in the study area for this project, located at the base of Fan 3.

3.3.2 Stratigraphy of Fan 3 in the study area

The stratigraphy of the Fan 3 lobe complex is presented Fig 3.13, as well as in correlation panels (Panels 1 through 12, Fig. 3.16 to 3.23; the legend for all the panels is displayed in Fig. 3.14; see Fig. 3.15 for panel locations). The stratigraphic correlation required lobes to be identified and mapped around the study area, and each lobe will be described in turn. Several interlobe, thin-bedded units were also identified.

Thin-bedded intervals

Consisting mostly of siltstone, the thin-bedded intervals were used to separate the individual lobes, as per the definition of a lobe (Chapter 2). Johnson *et al.* (2001) identified and described three types of claystone- and siltstone-prone units, marking varied periods of reduced sediment supply to the basin. Type 1 units represent long periods of hemipelagic deposition and are visible as interfan hemipelagic claystones, e.g. the 50 meter succession between Fan 2 and 3. Type 2 units separate the individual lobes. Type 3 units are intralobe units that separate individual beds and bed-sets.

The Type 2 siltstones were designated A through G, with A situated below Lobe 1 and G above Lobe 6. The latter is only rarely exposed, therefore the maximum thickness is unknown. Also, it is not an interlobe unit, as no lobe is present above it in the study area. Interlobe (IL) units C and D, situated below and above Lobe 3 to the north of the Gemsbok River, were combined in the southern outcrops, as the lobe is not present. Interlobe A, B, C+D, E and F reach maximum thicknesses of 0.3m, 0.3m, 2.71m, 0.84m and 1.62m, respectively along strike. Up-dip, IL A reaches 1.84m, IL B 1.57m, IL C+D 2.06m, IL E 1.05m, and IL F 0.72m. Minimum thicknesses were not determined as the interlobe siltstones are often eroded away by amalgamated sandstones. The Intralobe (IT) units that separate the Upper and Lower lobes were designated 1 to 4, with IT 1 between Sub Lobe 1 and 2, IT 2 between Upper Lobe 2 and Lower Lobe 2, IT 3 between Upper Lobe 4 and Lower Lobe 4, and IT 4 between Upper Lobe 5 and Lower Lobe 5. Along strike they reach 0.75m, 0.54m, 1.67m, and 1.05m, respectively. Up-dip

they reach thicknesses of 0.97m, 1.01m, 2.35m and 2.67m, respectively. Note that Interlobe A is situated between the sub lobes and Lobe 1. To the north, the sub lobes are not present, and the entire basal succession of siltstones is referred to as IL A. In this study, the section between the stratigraphic base of Fan 3 and the sub lobes is left unnamed, as this is interpreted to represent the onset of deposition.

Sandstone lobes

It should be noted that the descriptions of the lobes below indicate that some lobes were separated into lobe-elements. However, according to the definition of a lobe (sand units separated by thin-bedded, fine-grained intervals), the continuity of the intralobe siltstones, as well as the depositional patterns observed (Section 3.4 and Chapter 6), these “elements” should be classified as lobes. For the sake of simplicity, and to conform to the larger Lobe project, this distinction was not made. They were, however, treated as separate units for the modelling section of this project (Chapter 7).

The first (oldest) lobe at the base of the succession, Sub Lobe 1 (Lobe SL1), is not so much a singular lobe as a loose grouping of the first significant low-volume lobes (consisting of only single beds). It pinches out in only a few hundred metres along strike in the Gemsbok Valley. The unit can be traced up-dip all the way to the south of the study area. Several more sandstones appear up-dip, but the unit never forms a singular lobe. The second group of sandstones is closer to a lobe as defined above, as a clear siltstone break is present at the base and top. This unit, Sub Lobe 2 (Lobe SL 2), does not extend far eastward, but does remain fairly constant up-dip in terms of thickness, presence and lithofacies.

Neither of these units was identified to the north, and they are interpreted to pinch out across the two kilometre gap between the northern and southern outcrops of the Gemsbok valley. Also, no channelised areas were identified at outcrop. Either they are not present, or were located somewhere to the west (where no outcrop is present).

The next lobe, Lobe 1 (L1) is the first of the lobes that is also present to the north of the Gemsbok River valley. As in the northern outcrop, this lobe is not very extensive, reaching a maximum thickness of 4.5 metres. It pinches out over a kilometre along strike, and two kilometres down-dip. It does show a significant thickening towards the west at the start of outcrop, before the outcrop is lost.

Lobe 2 (L2) can be separated into two lobe-elements, namely an upper element (UL2) reaching 5.4 metres in thickness, and a much thicker lower element (LL2) reaching 8 metres. They are separated by Intralobe element 2. The quality of the outcrop makes this lobe particularly difficult to follow beyond its thickest section, roughly a kilometre from the western start of the southern outcrop in the river valley. Most of the lower section of the outcrop area is very poorly exposed laterally, making accurate correlation improbable.

Lobe 3, as identified to the north, is not present in the study area. Lobe 4 (L4) forms some of the most prominent outcrops and largest cliff faces (up to 13.5 metres at the thickest section). It can also be subdivided into two lobe-elements, namely Upper (UL4) and Lower (LL4) Lobe 4, separated by Intralobe element 3. The elements reach maximum thicknesses of 7.9 and 5.6 metres, respectively. Both elements show several thickening sections along strike. LL4 pinches out after 3.5 kilometres in an eastern direction, whilst UL4 is still present when the outcrop is lost to ground cover in the east. It becomes difficult to separate Lobe 4 into different lobe-elements up-dip.

Lobe 5 (L5) also consists of two elements, Upper (UL5) and Lower (LL5) Lobe 5, separated by Intralobe element 4. These lobe-elements differ from the other lobes in that they show completely different depositional patterns. The two elements should probably be treated as separate lobes. However, in order to conform to the observations of the larger Lobe project's observations, the elements were left as part of the same lobe. LL5 is present for the whole length of the study area along strike, reaching a thickness of 10.9 metres down-dip and 4.9 metres along the Gemsbok River valley. UL5 reaches 5 metres down-dip, and 3.3 meters along the Gemsbok River valley. UL5 pinches out in about 2 kilometres eastward along the valley. Again, up-dip it becomes almost impossible to separate the elements. Lobe 5 only appears again 2 kilometres down-dip.

Lobe 6 only appears in outcrop about 500 metres from the start of the Gemsbok River valley's outcrop in the west. It gradually thickens towards the east, until it is also lost to ground cover. It reaches a thickness of 9.2 metres near the end of the outcrop in the east at Rondavel 34, where the lobe's only identified channelised zone is present. Only a very small portion of Lobe 6 is visible down-dip at the most southern outcrops of the study area (Panel 12).

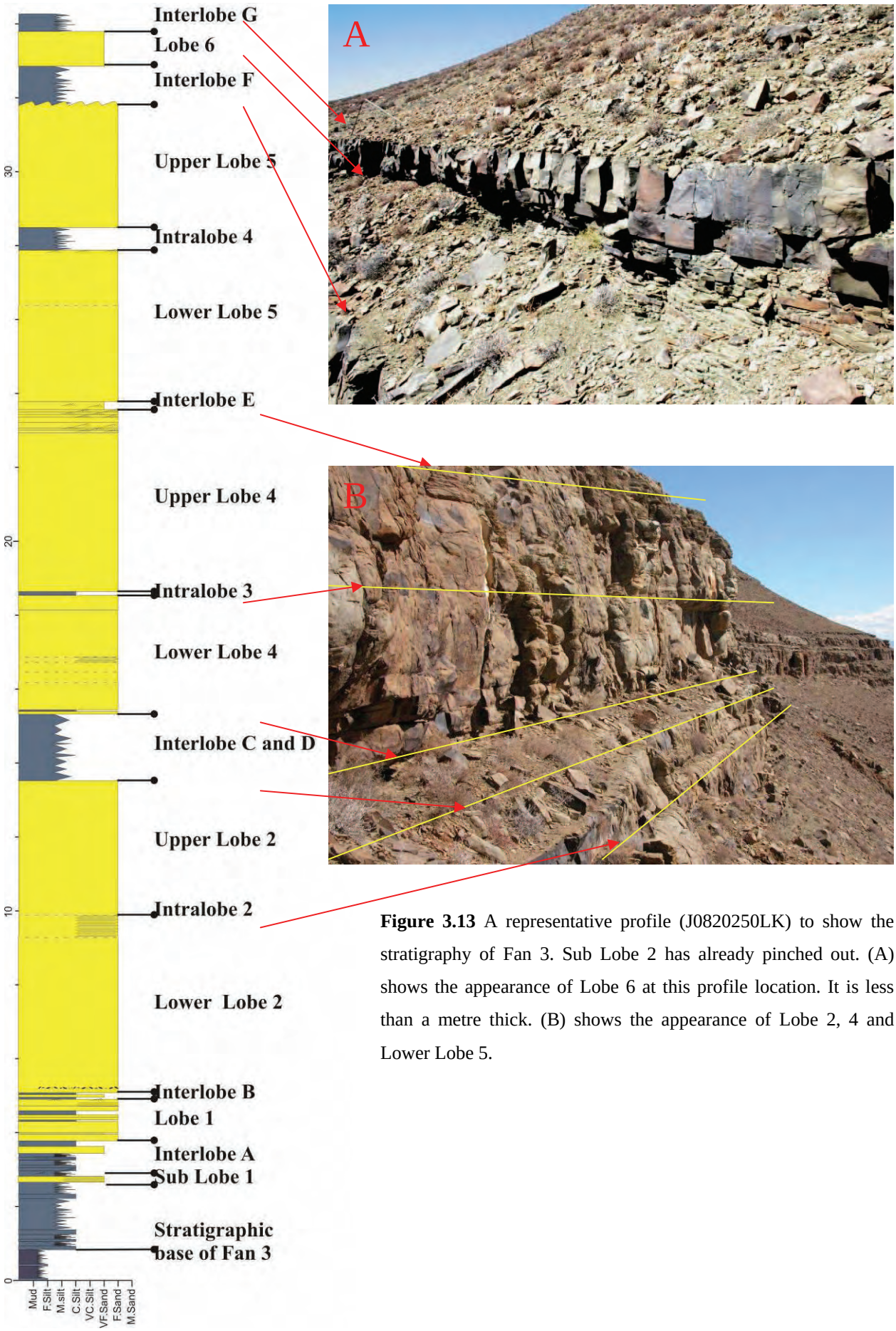

Figure 3.13 A representative profile (J0820250LK) to show the stratigraphy of Fan 3. Sub Lobe 2 has already pinched out. (A) shows the appearance of Lobe 6 at this profile location. It is less than a metre thick. (B) shows the appearance of Lobe 2, 4 and Lower Lobe 5.

3.4 Architecture

3.4.1 Introduction

The architecture of a distributive deep-water system is determined by several factors. These include flow direction, the presence or absence of channels, barriers (e.g. topography, previous lobes), and the strength and density of depositional flows. In a fan as large as Fan 3, these factors can be applied to each individual lobe or lobe-element. Architectural elements include channels, sheets and transitional elements in between.

Channels are relatively easy to identify: they are typically large, concave structures that scour into the underlying lithologies, generally associated with large amounts of MCCs. They are commonly found closer to the proximal parts of a fan, and can form stacked channel complexes (Fig 1.3). Channels are generally lobe-scale features, although smaller lobe-element-scale channels may be present. Johnson *et al.* (2001) identified five different channel types, based on geometry and fill style. These include erosional channels with complex fills (often with significant lag deposits formed by sediment bypass) and composite margins; erosional channels with simple fills and margins; channels with only minor scouring at the base (more deposition than erosion); erosional channels characterised by heterolithic thin-bedded fills; and channel complexes. Channel fills can include most of the other channel types.

If they are present, channels generally do not extend far into distributive systems. In mid-fan areas, depending on the strength of the depositional flows, channels commonly grade into what are called channelised sheets or highly amalgamated zones (Hodgson *et al.*, 2006). These zones do not show a great deal of scouring (generally less than a metre), instead loading is more common. This loading can extend several metres below the channelised zones, causing compression and loading of the lower lithologies. These often follow the base of the amalgamated zones at a fixed distance.

Channelised zones are rare in distal areas where sheet deposits with planer upper and lower surfaces are common. They can be either amalgamated or structured. In the Gemsbok River valley (strike section through mid Fan 3), the channelised sheets are both lobe- and lobe-element features (down-dip extensions of channels). Sheet deposits fill the area between the channelised

sheets. These sheets can be anything from lobe-scale features to bed-set features, depending on their relative position to an axial zone and the thickness of a lobe.

Palaeocurrent measurements provide an important constraint in determining the depositional environment of a submarine fan (e.g. flow direction and strength), as well as constraining the 3D shape of a lobe or lobe-element. Palaeocurrent indicators include current ripple laminations, parting lineations, and sole structures. All palaeocurrent measurements within a lobe-element are grouped together to give an indication of the behaviour of a specific lobe.

The panels below provide information of the architectural behaviour of the stratigraphic units in 2D space. Panels 1 – 2, 3 and 3 – 4 are oblique strike sections along the mid-fan area (i.e. the Gemsbok River valley). Panel 12 is a dip-section roughly along the fan's axis. The other panels are small strike sections along the length of Panel 12.

The "Panel X – Y" names represent sections where two originally separate panels were either combined (1 – 2, 8 – 9 and 10 – 11) or where a smaller section intersects a larger one (3 – 4).

Short notes are presented on each panel, focussing on important details found on each panel.

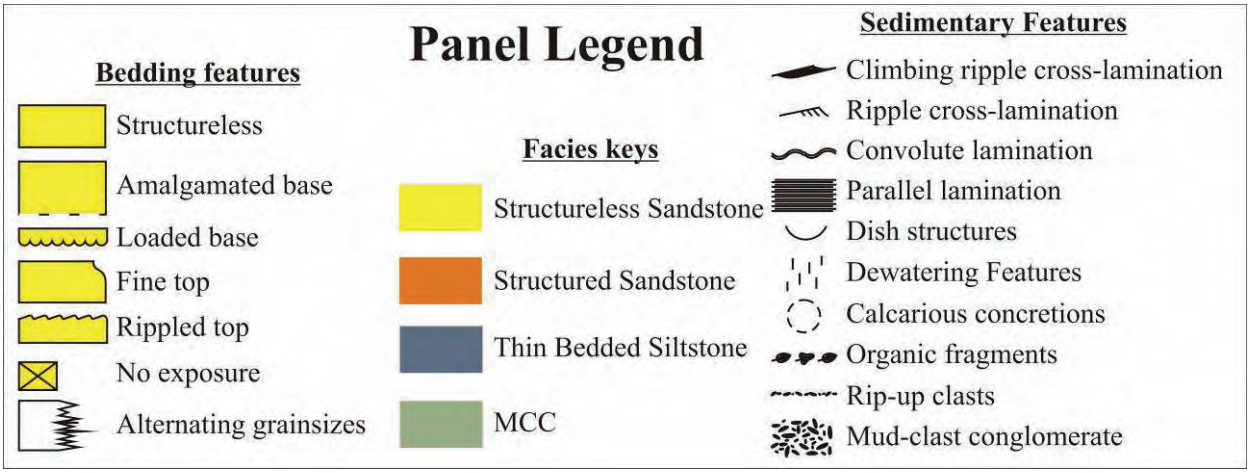

Figure 3.14 Legend for all the correlation panels.

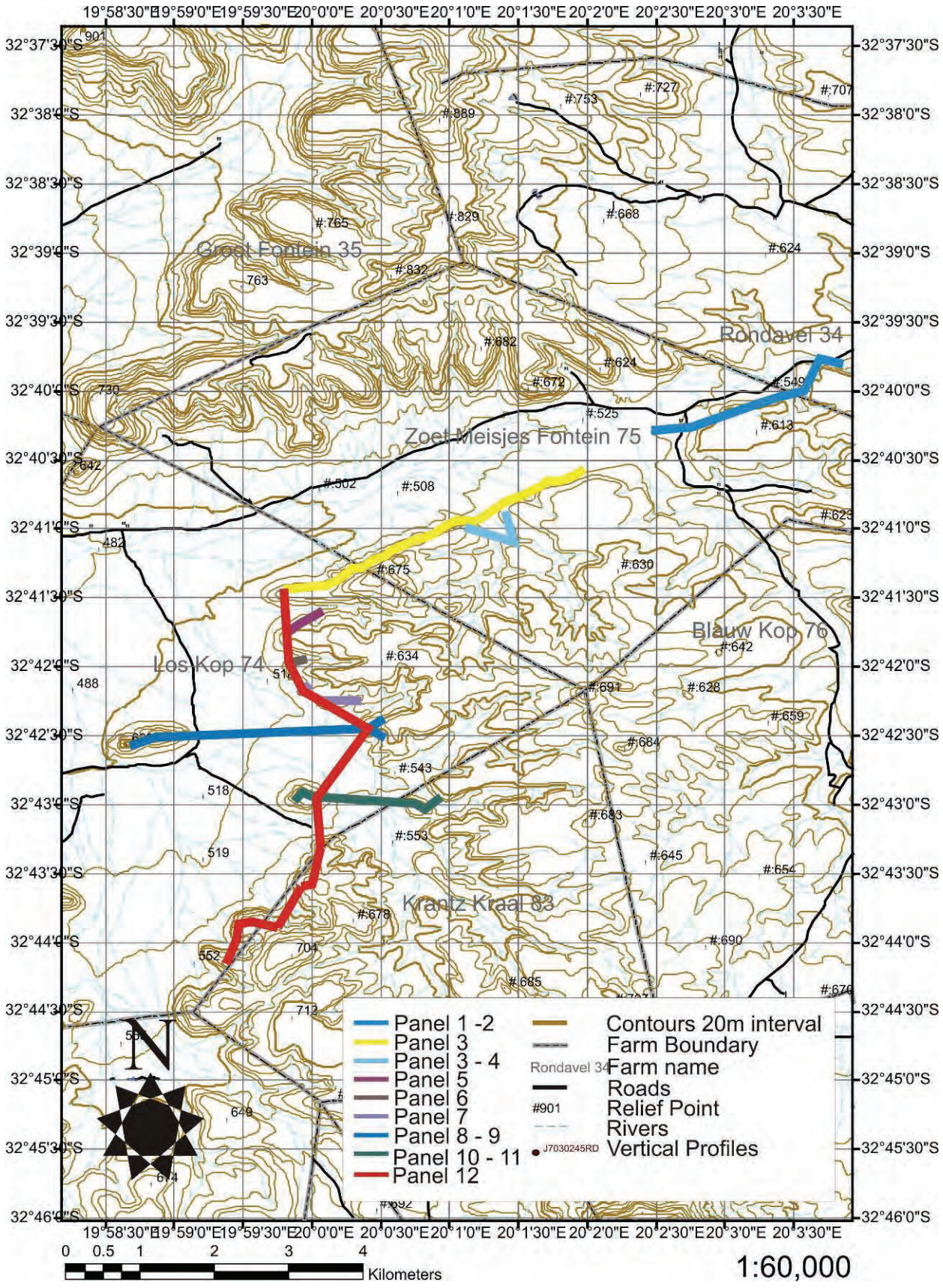

Figure 3.15 Topographical map of the area indicating the locations of the various correlation panels.

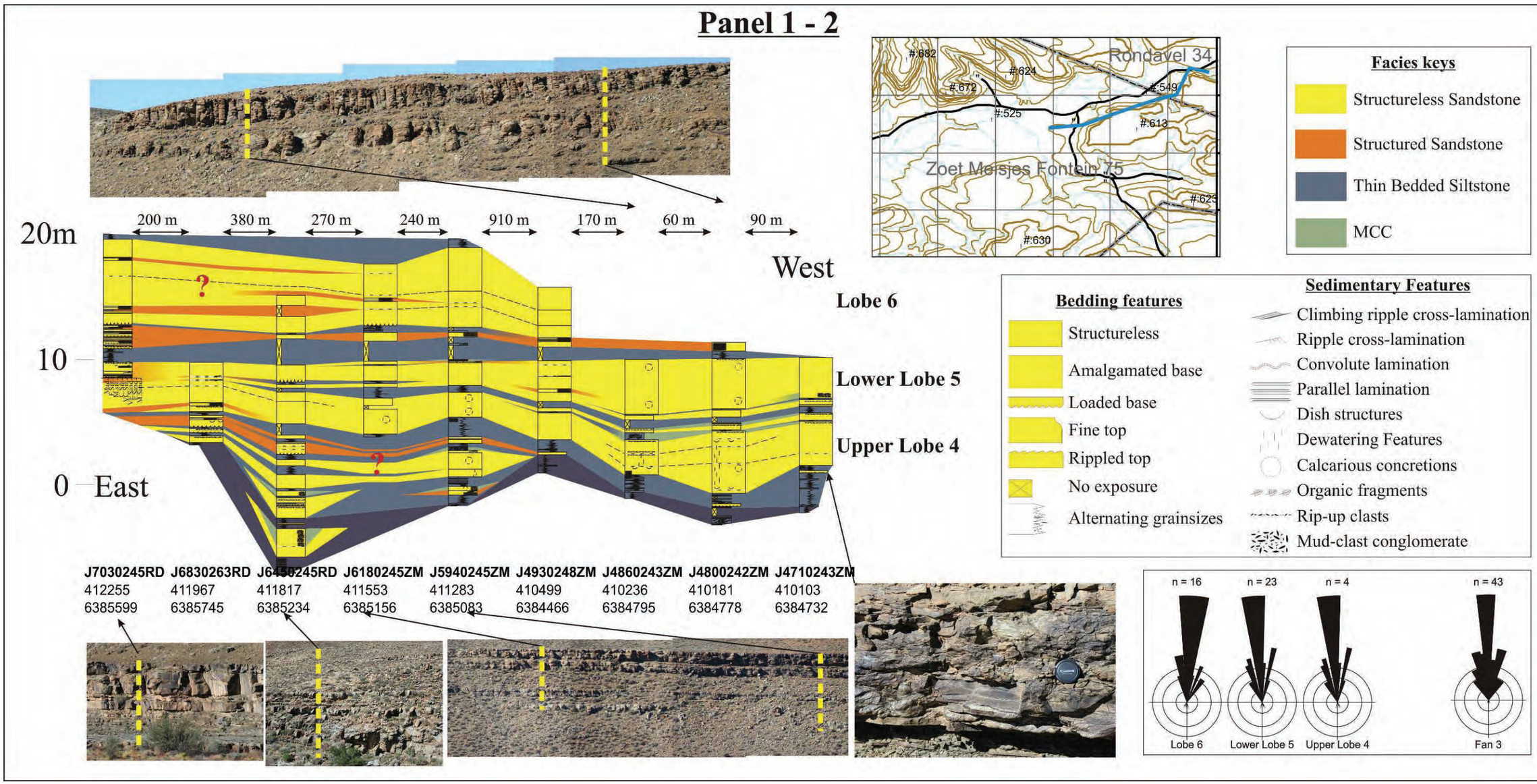

Figure 3.16 Panel 1 - 2. Fan 3 disappears into the ground a few hundred metres to the east of the last profile.

Notes on Panel 1 – 2

Panel length is 2320 metres. The eastern end of the panel is the end of outcrop for Fan 3. A hundred metres southeast down the valley, the top 3 metres of Lobe 6's axial zone is still exposed. A significant (more than 8 metres) of "extra" outcrop is present around 6450m to 5940m. This possibly represents a marginal finger deposit of Lower Lobe 4, which already pinched out two kilometres to the west (see Chapter 6 for a detailed discussion of the finger-shapes deposits). Upper Lobe 5 pinched out 3.5 kilometres to the west. 4930m to 4710m represent another finger-shaped deposit, this time for Upper Lobe 4. It shows significant thickening, followed by rapid thinning (thins to less than 1 metre in 100 metres before thickening towards 4930m). It also displays many dewatering features (indicating rapid deposition) and large volumes of MCCs.

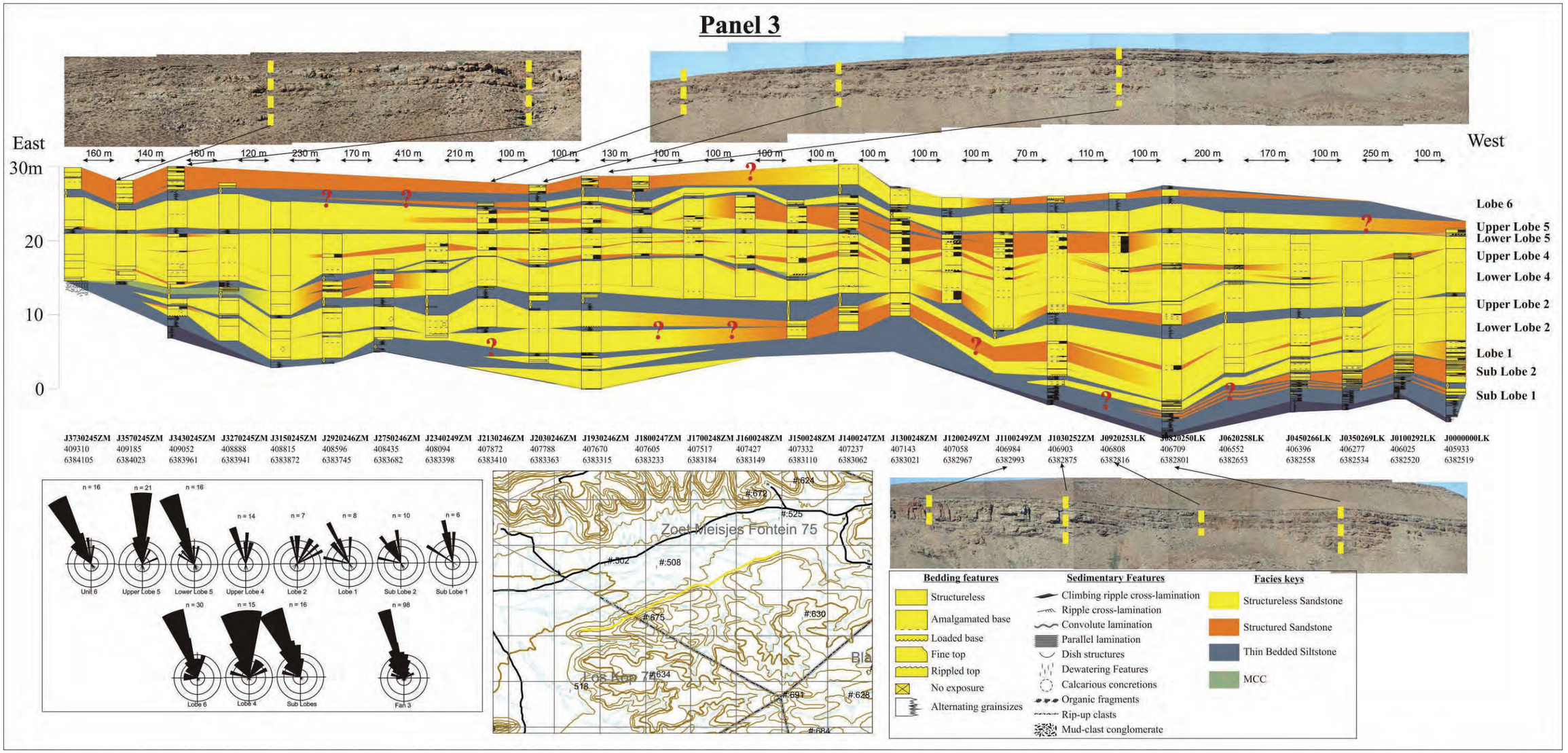

Figure 3.17 Panel 3. The most continuous section of outcrop in the field area is the first 2.3 kilometres to the west of this area. It represents the southern Gemsbok River Valley outcrop of mid-fan Fan 3.

Notes on Panel 3

Panel length is 3780 metres. Lobe 6 remains structured for almost its entire length. Upper Lobe 5 remains structureless, safe for its pinch-out at 2130m and the western start of outcrop. The largest of the channelised areas is located between 450m and 1200m. Lower Lobe 5 and Lobe 4 all thicken significantly. Lower Lobe 5 has axial zones located at 450m, 1700m, and 3270m. Upper Lobe 4 has axial zones at 1030m, 1500m and 3150m. Lower Lobe 4's axial zones are at 1100m and 1700m, with its pinch-out at 3270m. Note the MCCs located at this point. Lobe 2 thins significantly beyond 1030m, but thickens again at 1930m. Lobe 2 has axial zones at 0820m, 2030m and 2920m. It is not certain where the extra section below Lobe 2 at 1930m belongs in the stratigraphy. Lobe 2 pinches out relatively rapidly past 3270m. Lobe 1 pinches out at 1030m, Sub Lobe 1 at 0820m, and Sub Lobe 2 at 0450m.

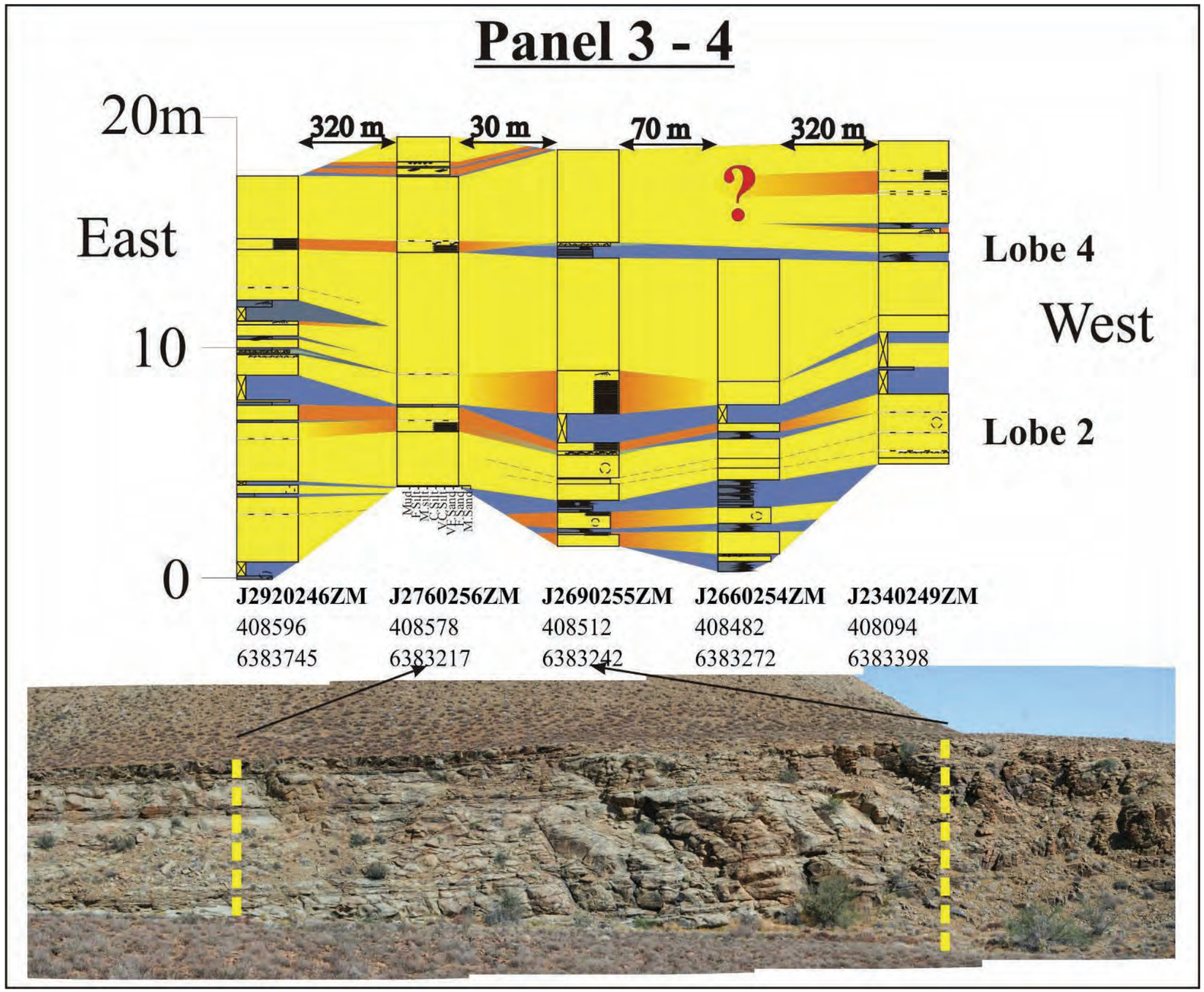

Notes on Panel 3 – 4

Panel length is 580 metres. The two profiles on the sides, J2920246ZM and J2340249ZM, are part of Panel 3. The western correlation of Lower Lobe 4 between J2660254ZM and J2340249ZM can be walked out. This panel represents a down-dip continuation of the channelised areas identified to the northeast on Panel 3, at profile J3150245ZM. Some MCCs are located close to local amalgamation zones at 2690m.

Figure 3.18 Panel 3 - 4. This section of outcrop lies slightly to the south of Panel 3. The two edge profiles are part of Panel 3.The western correlation with Fan 3 can be walked out.

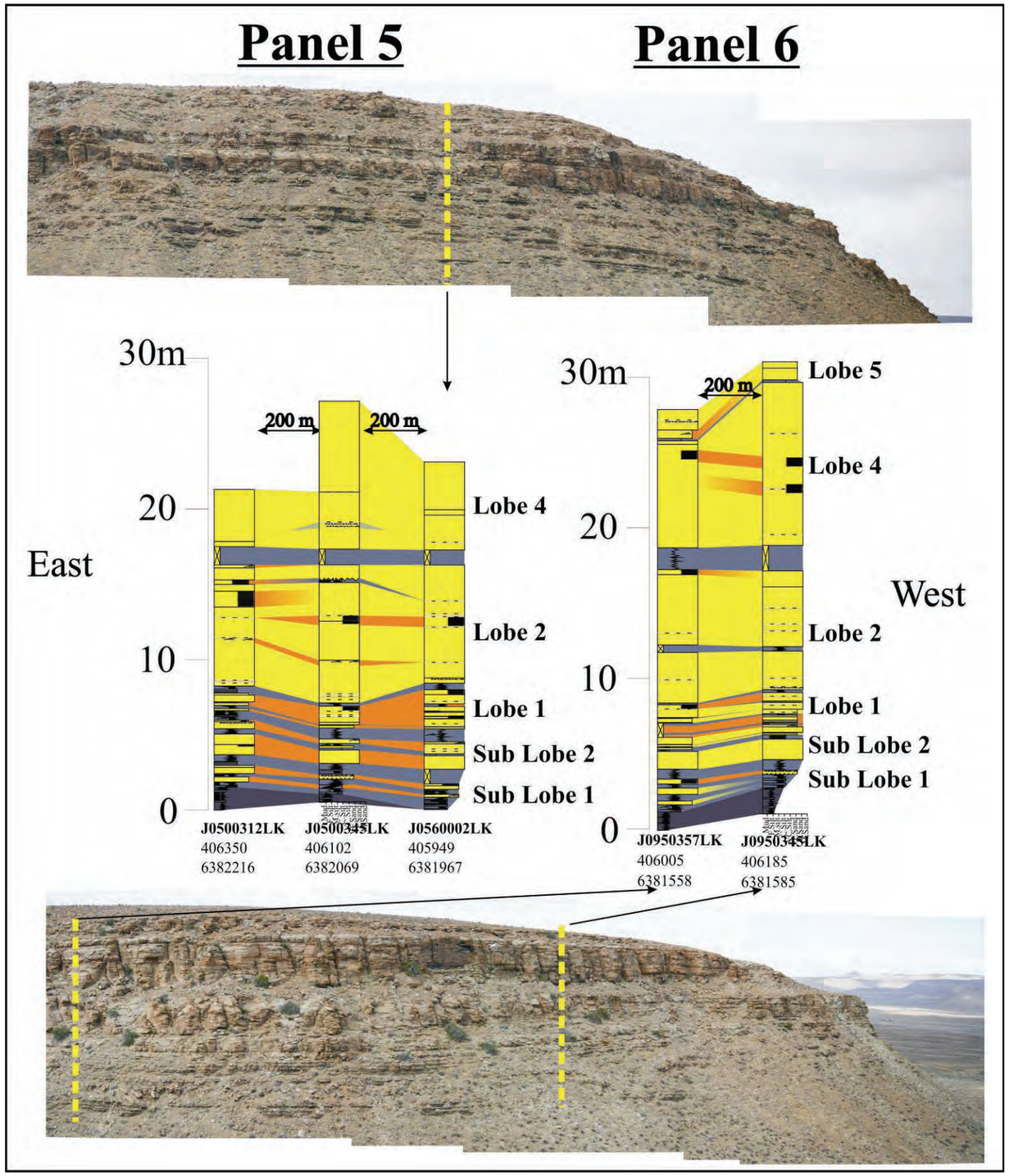

Notes on Panel 5

Panel length is 400 metres, and is located 500 metres south of the western end of Panel 3. Lobe 1 is very structured and bedded, as it is 500 metres to the north.

Notes on Panel 6

Panel length is 200 metres. The first of several pinch-outs of the lower part of Sub Lobe 1 is visible here. Only the upper part of Sub Lobe 1 is continuous up-dip. Lobe 1 is still very bedded and structured.

Figure 3.19 Panels 5 and 6. They represent the first two valleys south of the Gemsbok valley. From Panel 5 onwards it becomes increasingly difficult to correctly correlate the Panels, as the outcrops become poorer and further apart.

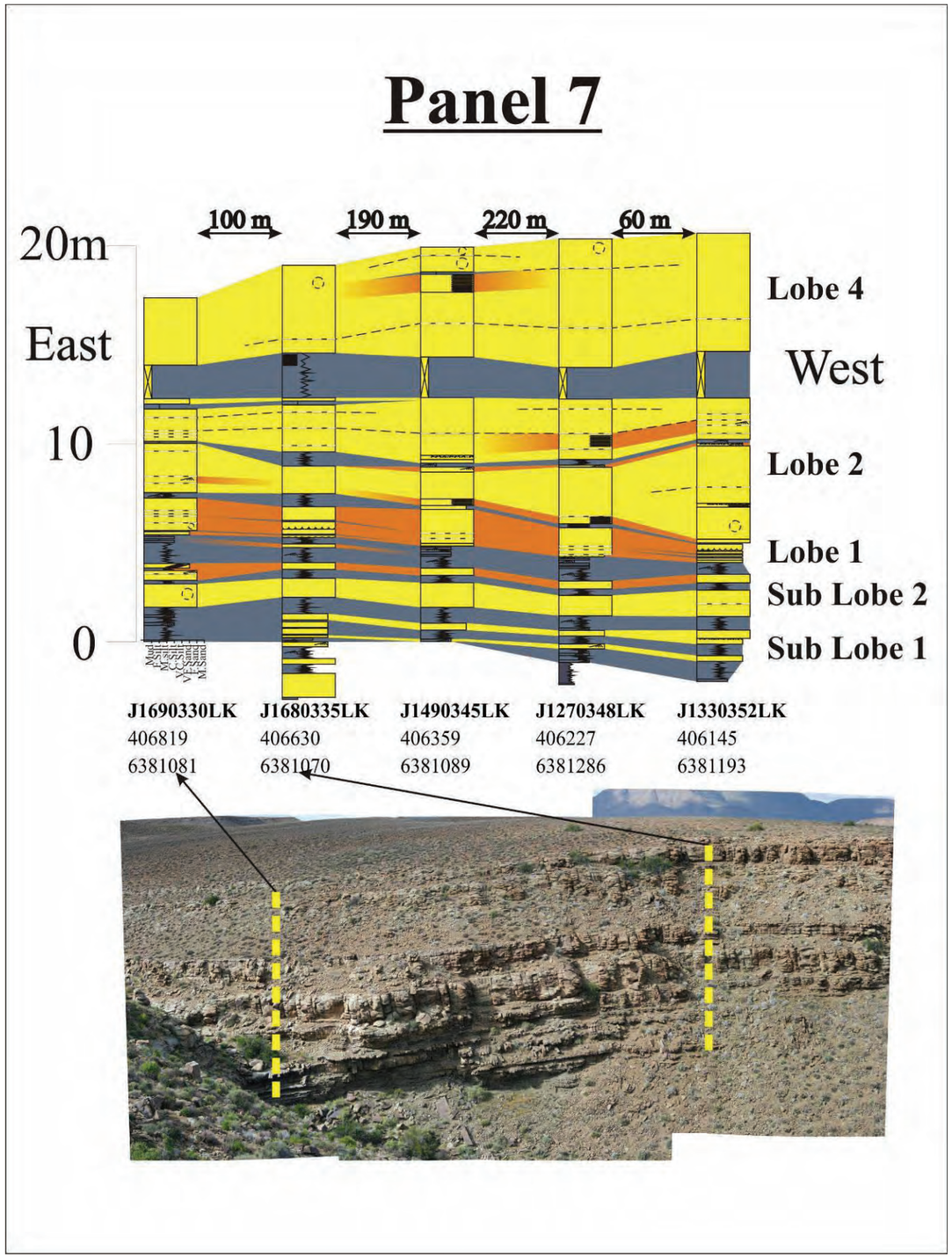

Notes on Panel 7

Panel length is 570 metres. Interlobe C and D is at its thickest in the up-dip direction around J1680335LK. The panel is located within the thinnest section of outcrop, where all lobes show significant thinning (see Panel 12). This section is generally well structured and bedded.

Figure 3.20 Panel 7. Panel 7 is not truly a "straight line correlation, but rather a correlation around a bend in the outcrop. The two sides of the headland were close enough together to warrant the above correlation.

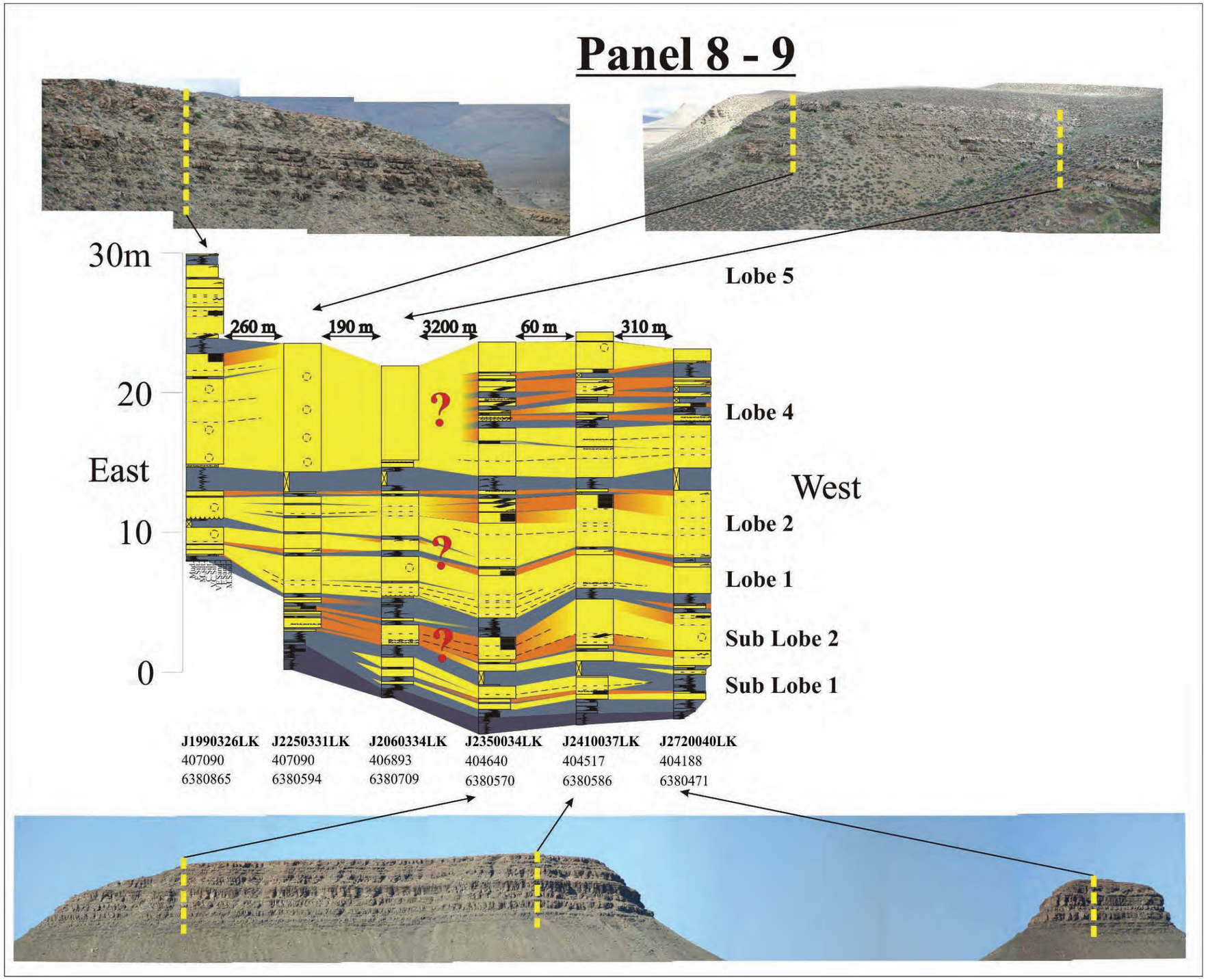

Notes on Panel 8 – 9

Panel length is 3830 metres. The western profiles represent the western most of all profiles, located on the Los Kop Twins. The outcrops are mostly ripple laminated, and are probably not situated close to a major axial zone. The Twins are located 3.2 kilometres from the nearest eastern outcrops, making correlation difficult. If correct, it supports the inferred positions of the axial zones of the sub lobes, as well as Lobe 1, located well to the west of the Gemsbok River valley.

Figure 3.21 Panel 8 - 9. The Los Kop twins (bottom photo) are situated some three kilometres away from the nearest correlatable outcrop to the east. As such the only a general correlation could be safely attempted.

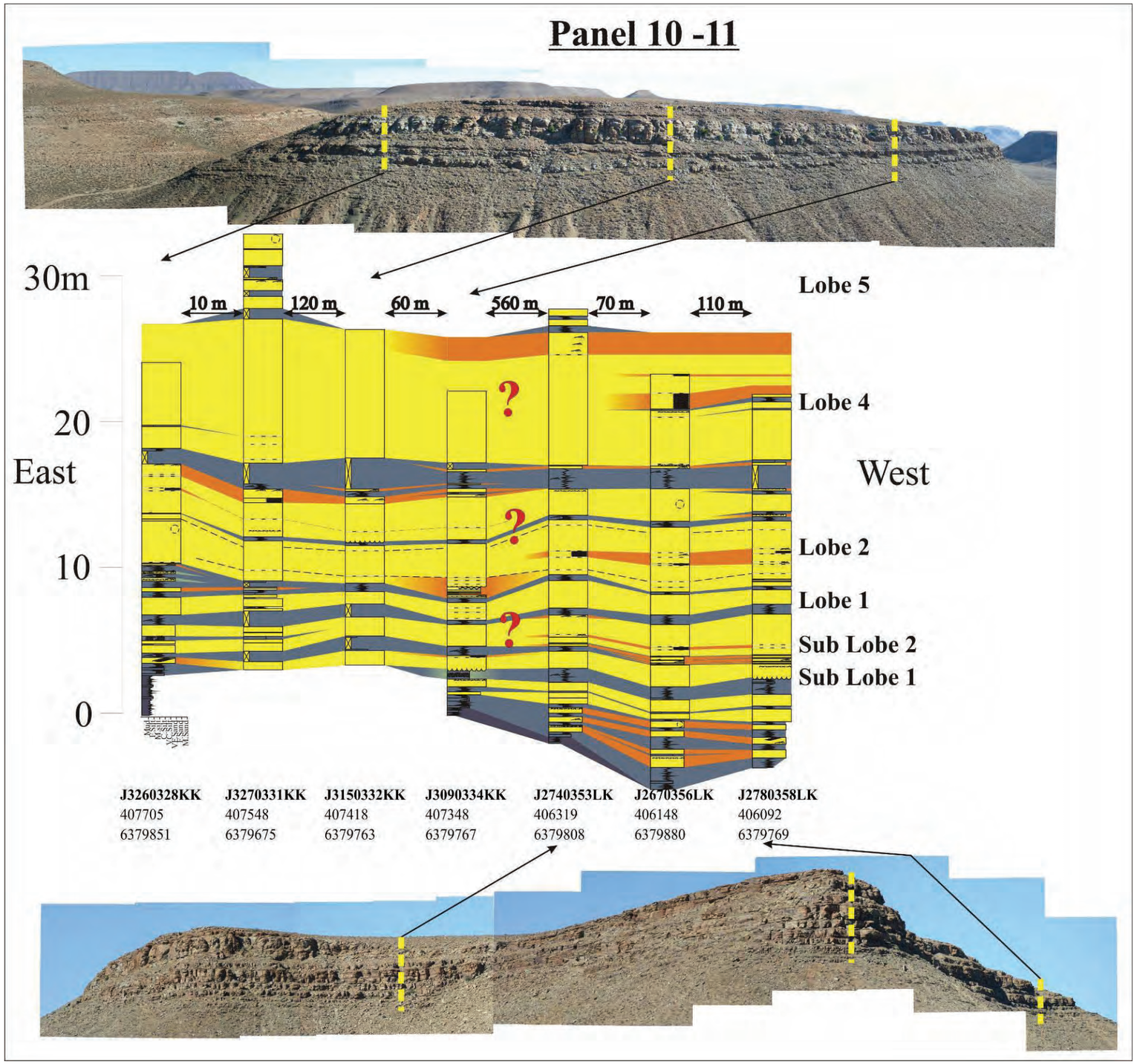

Notes on Panel 10 – 11

Panel length is 930 metres. The interbedded sandstones of Interlobe C and D start to appear here. An axial zone of Lobe 4 is located at J3270331KK. This area is nearing the pinch-out of Lobe 1.

Figure 3.22 Panel 10 - 11. The southern most strike section. Again, most of the outcrop is located on isolated hills several hundred metres from the nearest correlatable outcrop.

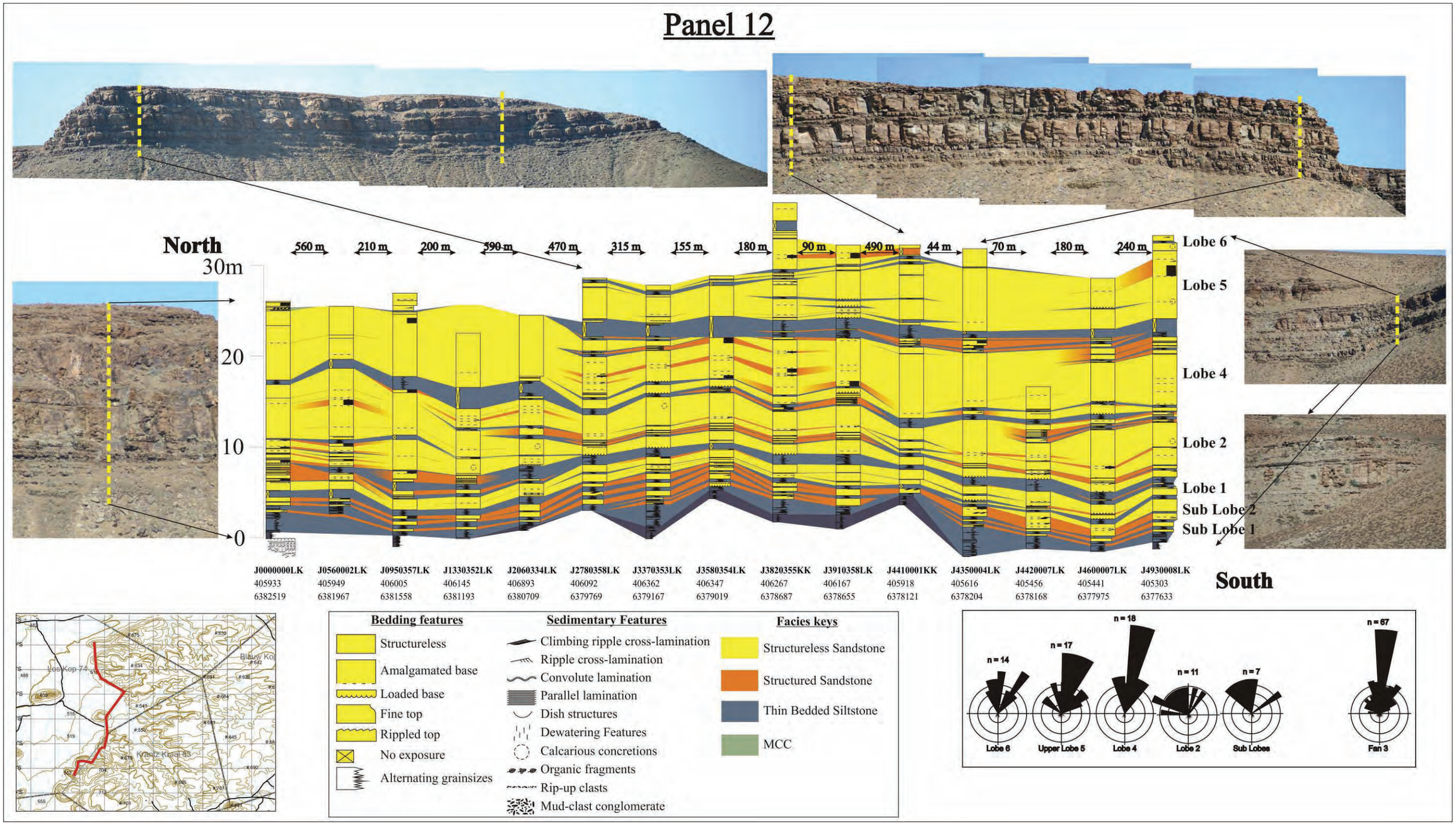

Figure 3.23 Panel 12. A 4.9 kilometre north-south trending dip-section from mid-fan (north) to more proximal (south).

Notes on Panel 12

Panel length is 4930 metres. All lobes show a thinning pattern between 2780m and 3820m. The panel runs almost parallel to an axial zone of Lobe 4 between 0m and 2060m, and between 4410m and 4420m. Interlobes C and D, as well as E show significant thickening down-dip (south) and become interbedded with thin-bedded sandstones. Lobe 1 pinches out at 2060m.

3.4.2 Architecture of mid-fan Fan 3

Palaeocurrents

Figure 3.24 is a summary of palaeocurrent directions measured during previous studies. Figure 3.25 shows the summary of the palaeocurrent measurements for the whole of Fan 3 in the study area (A), as well as the summaries for the main lobes and lobe-elements (B). Combined with the data gathered from previous studies, a pattern of distribution directions could be determined for Fan 3. The general spreading pattern of the lobes should already be evident from Fig. 3.25.

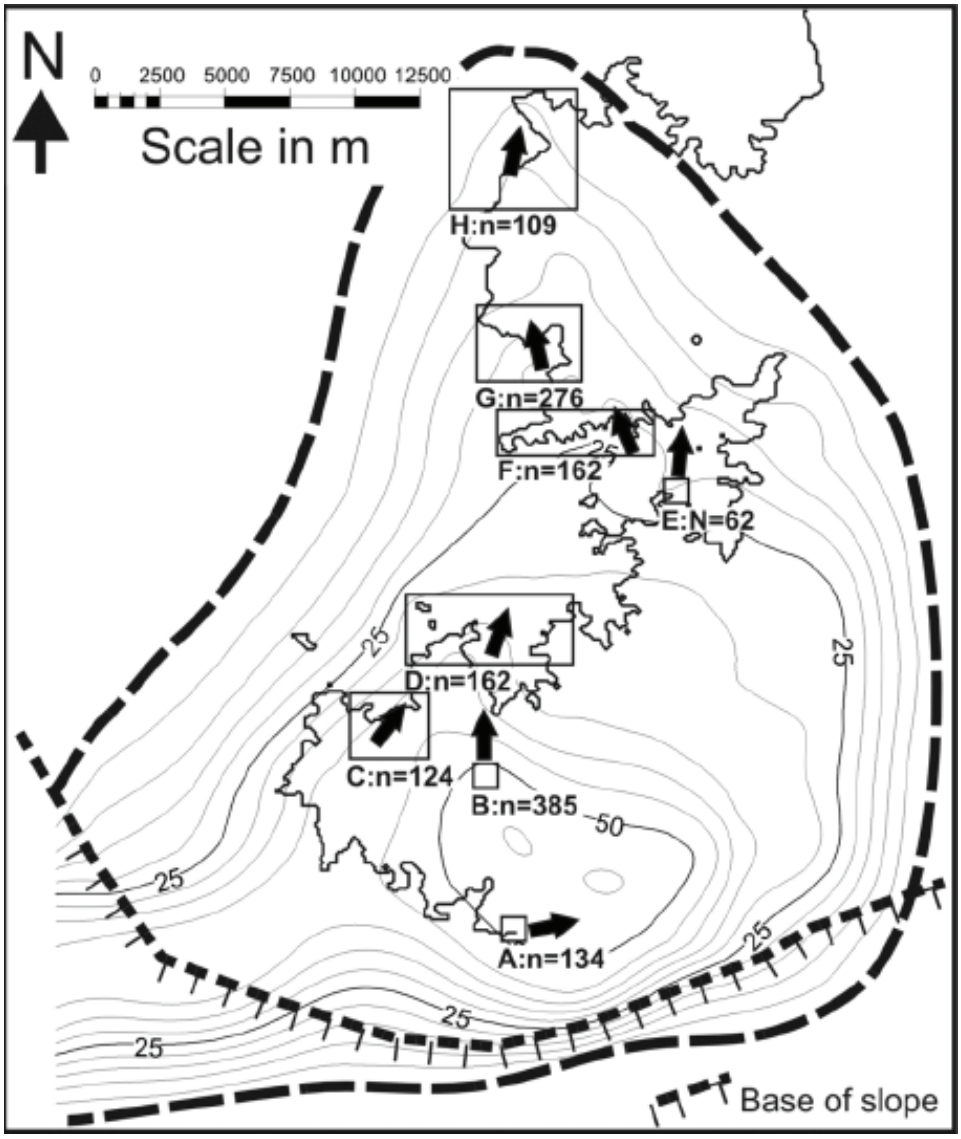

Figure 3.24 Averaged palaeoflow directions measured for Fan 3 in previous studies. From Hodgson *et al.* (2006)

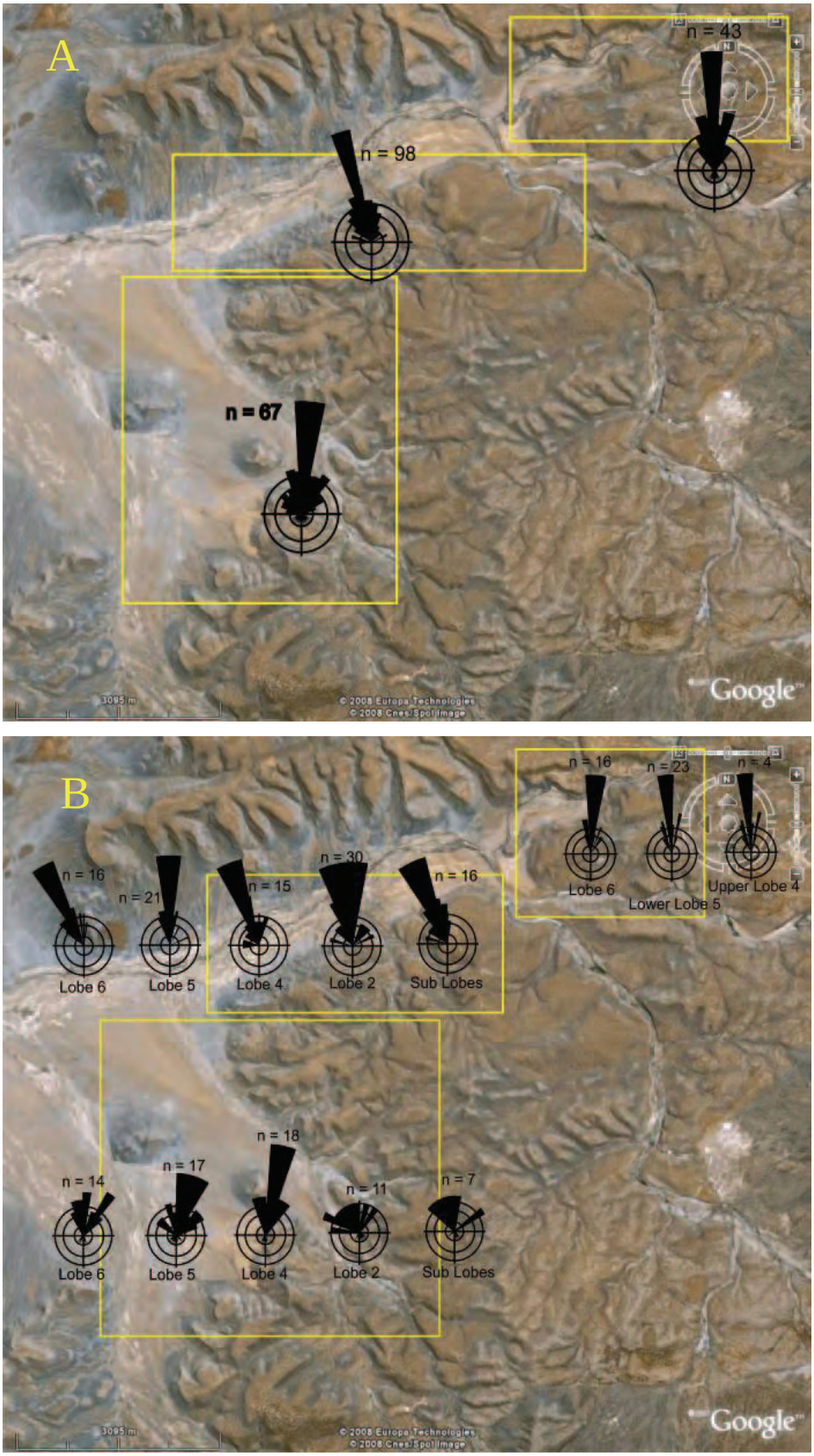

Figure 3.25 Palaeoflow directions for Fan 3. (A) is a summary of the whole Fan 3, whereas (B) breaks down the palaeoflow into the main lobes. The yellow blocks represent the areas from which the groups of palaeoflow indicators were taken. The majority of the palaeoflow indicators are ripple laminations.

Across the study area, Fan 3 changes direction from north of northeast in the south to north of northwest in the north in just over four kilometres. It continues in a northerly direction closer to the margin of the Fan. This is of course only a compilation of data across different parts of the fan. There is a great deal more variation at the lobe and lobe-element levels, which is described below.

No channels were identified in the study area, though several channelised or highly amalgamated zones were identified. Axial zones, in this project, refer to zones of focussed flow, not necessarily the central axis of a lobe or lobe-element. Indeed, some lobes contain more than one of these zones.

Sub Lobes and Lobe 1

Description:

The sub-lobes, as well as Lobe 1, show no real variation in their north-westerly course, although a focussing of the flow direction seems to occur towards the north. This is probably due to the fact that they are nearing their distal margin, as they barely reach the northern outcrops of the Gemsbok River valley before they pinch out. As stated above, only Lobe 1 is present to the north, and only for a short distance. No major channelised areas are observed. Lobe 1 quickly pinches out up-dip. An interesting observation is that the Sub Lobes are present for the entire length of Panel 12.

Interpretation:

The palaeoflow directions, combined with the small spatial extent of Lobe 1, suggest that it might only be a localised feature. Palaeocurrents don’t support this being the distal margin of a lobate body, unless the axis flowed in an almost western direction. The thickening of Lobe 1 towards the west suggests the presence of an axial zone probably within a few hundred metres to the west. In terms of the spreading pattern normally associated with lobate bodies, it is unlikely that this is the margin of such a feature, unless the palaeoflow was almost due west. It is possible that Lobe 1 represents the initial phase of Lobe 2, deposited into a topographic low, ahead of the larger, more voluminous flows. The palaeocurrents support this to some degree, as they almost exactly match the palaeoflow direction of Lower Lobe 2. Also, the amalgamation of Lobe 1 and Lower Lobe 2 near the start of outcrop adds additional support, especially as this is also an axial zone for Lobe 2.

Lobe 2

Description:

Lobe 2 shows a dispersive pattern in its palaeocurrents, as they vary with more than 90 degrees. Palaeoflow is mostly focussed north of northwest in the north, but has a more general north-western pattern to the south. Lower Lobe 2 shows a more north-western flow pattern, whereas Upper Lobe 2 often shows a much more easterly flow direction in the mid-fan area. Lobe 2 shows only 2 major thickenings before it disappears from outcrop for several hundred metres along strike. The first is located at the start of outcrop in the Gemsbok River valley, in Lower Lobe 2 (western end of Panel 3, northern end of Panel 12). This zone amalgamates Lower Lobe 2 to Lobe 1. Lower Lobe 2 thins slightly as Upper Lobe 2 begins to thicken, but thickens again 500 metres to the east. Correlatable outcrops are absent for more than a kilometre. Lobe 2 has already begun to thin significantly at this point, and pinches out over the next kilometre.

Up-dip, Lobe 2 slowly thins for the first 3 kilometres, but gradually thickens again for the remainder. At 1.3 kilometres (Panel 7) Lobe 2 rapidly thins to the east at 0.5 metres every 100 metres. The same thinning is observed a kilometre further south (Panel 8 – 9). However, at 3.3 kilometres south (Panel 10 – 11), Lobe 2 has a relatively constant strike thickness.

Interpretation:

Lobe 2 displays only two zones of focussed flow in the study area. The dispersive pattern can probably be attributed to a more even topography healed by Lobe 1, allowing the lobe to spread more widely. Lobe 2 is also the first lobe to display what appear to be the “finger-like” axial zones. It is difficult to accurately trace along strike, due mostly to missing outcrop.

At about 2 kilometres east from the start of the Gemsbok River valley, a significant “extra” section is present at the base. While modern land slides do represent a problem in the field area, this feature is unlikely to be one, as it displays none of the features associated with slumps (e.g. duplication and lateral discontinuity of bedding). The palaeoflow directions, as well as the bedded nature of the thinner up-dip section of Lobe 2 both support the interpretation of this area being an off-axis section. In other words, this is parallel to the curve observed in the palaeocurrents measurements, and the bedded nature indicates an area removed from an axial

zone. Lobe 2's thinning rate towards the east at 1300 m south infers the lobe margin some 500 metres farther east, assuming no finger-shaped zones are present.

Lobe 4

Description:

Spatially and volumetrically, Lobe 4 is the largest of the lobes. The palaeoflow direction is more focussed, and shows a trend matching that of Fan 3. Given its size, it still shows considerable variation, but a general flow direction to north of northeast in the south, shifting to northwest in the north, is observed. The spreading effect at the edge of lobes can be observed towards the east, as the palaeoflow direction here starts to verge towards the north.

Several channelised zones are present within Lobe 4. Four of these zones can be identified in Panel 3, the last occurring in Upper Lobe 4 just before Lower Lobe 4 pinches out. Upper Lobe 4 shows one more major thickening before outcrop is lost to ground cover (western side of Panel 1 - 2). At this point, Upper Lobe 4 thickens some 8 metres in less than 100 metres, and displays large amounts of mud-clast conglomerates at the top of the sandstone beds. This location also displays major dewatering features, but only a small amount of scouring at the base.

A similar feature is present below Upper Lobe 4 a few hundred metres towards the west of the above mentioned feature. Here the outcrop is more bedded, also featuring a large amount of mud-clast conglomerates at the top and above the thicker sandstones.

Up-dip, Lobe 4 maintains a fairly constant thickness. It becomes much more bedded towards the south, with one channelised area near the southern-most edge of the field area (eastern side of Panel 10 -11). The Los Kop twins (western Panel 8 – 9) sees Lobe 4 become very structured and bedded.

Interpretation:

The focussed palaeoflow pattern is probably due to the fact that Lobe 4 is one of the last lobes to pinch out to the north. In other words, it had a stronger flow strength, and dispersed later than Lobe 2.

All of the thickened sections of Lobe 4 show a compensating pattern between the two lobe-elements along strike (Panel 1 – 2 and 3). The large volume of Lobe 4 suggests several scenarios for the depositional patterns identified in the study area. One scenario is that the lobe has more freedom to disperse than previous lobes, due mostly to infilling of the topography by previous lobes. Another scenario is that the flows depositing the lobe possessed more energy than previous lobes, allowing more sediment to be transported before being deposited. A third scenario is a decrease in accommodation in the basin, forcing basinward stepping (Lobe 4 is the last lobe to pinch out to the north). Yet another scenario involves all aforementioned scenarios, or any combination thereof. Given the presence of several axial zones, the likely scenario was a drop in relative sea-level, accompanied by an increase in sediment supply. Lobe 4 is also one of the last lobes to pinch-out to the north, suggesting a stronger palaeoflow, enforced by the basinward stepping.

If the pattern suggested by Machado *et al.* (2004) holds, it is highly likely that the extra section below Upper Lobe 4 is Lower Lobe 4. This pattern gives lobes a more "finger-like" appearance near the distal and fringe sections, as opposed to a strictly lobate shape (see Chapter 6 for a more detailed description of this feature). It has been confirmed by researchers from Liverpool University that the channelised zones become similar features to the north.

Lobe 5

Description:

Overall, Lobe 5 shows a similar axial pattern to Lobe 4, namely north-eastern palaeoflow in the south and north-western palaeoflow in the north. Several thickenings are observed along strike in Lower Lobe 5, all compensating with thinner parts of Upper Lobe 4. For the most part, however, Lower Lobe 5 remains mostly parallel-laminated, only becoming more structureless to the east, and then only for about 1.5 kilometres.

Upper Lobe 5 thins at a rate of 0.2 metres every 100 metres to the east. Upper Lobe 5 already pinches out 4 kilometres before the eastern edge of the study area. It is therefore not surprising to see a mostly northern palaeoflow direction in the Gemsbok River valley. Upper Lobe 5 maintains an amalgamated appearance all the way to pinch-out. No channelised zones are observed in Upper Lobe 5.

It is difficult to follow Lobe 5 up-dip, and near impossible to separate its elements. Overall, it thickens significantly up-dip, and also becomes more bedded. No strike up-dip section contains more than one profile with Lobe 5 exposed, therefore the east-west behaviour of Lobe 5 in an up-dip direction cannot be determined.

Interpretation:

Upper Lobe 5's thickening to the west suggests the presence of an axial zone somewhere between the start of outcrop in the Gemsbok River valley and the Los Kop twins.

Lobe 6

Description:

Lobe 6 shows the most variation of all the lobes, mainly because the western pinch-out of Lobe 6 lies about 500 metres east of the mouth of the Gemsbok River valley (Panel 3). The only identified axial zone for Lobe 6 lies 7 kilometres to the east (100 metres southeast of Panel 1 – 2), at the edge of the study area where Fan 3 is lost in outcrop. Only the top 3 metres of the axial zone is exposed. Lobe 6 also shows a northern palaeoflow direction here, but this is because flows were in a north-eastern direction in the south, then turned north as flows moved eastward. It thins to the west at a rate of 0.14 metres per 100 metres.

Lobe 6 is too poorly exposed up-dip for a correlation.

Interpretation:

Lobe 6's more easterly palaeoflow direction, as well as its completely offset position in relation to the previous lobes, suggests a slight shift of the feeder zone for the fan. The northward shift in its palaeoflow pattern again suggests the presence of some unidentified topographical barrier to deposition to the east and south. Lobe 6 also does not display the "finger-like" features of Lobes 2 and 4 in the study area. It simply displays "classic" lobe features, with a single main axial zone to the east, and a steady spreading pattern away from it.

Interlobe Units

Although these are not lobes, they still display some important features, especially up-dip. Here they start to see an increase in grain-size from silt to fine-sand, in some cases even merging

with the bounding sand-prone lobes. Interlobe element E is one such example (Panel 12). It has been suggested by Hodgson (personal communication) that these could possibly represent the margins of interlobe sand-rich units, or even lobes. If Lobe 3 is an example, then this is very possible. Unfortunately, outcrop in the area does not allow easy confirmation of this.